2018-07-23

Exploring the Role of ATF4 in Circadian Photic Phase Shifting

Chan, Ryan K.

UNIVERSITY OF CALGARY

Exploring the Role of ATF4 in Circadian Photic Phase Shifting

by

Ryan K. Chan

A THESIS

SUBMITTED TO THE FACULTY OF GRADUATE STUDIES

IN PARTIAL FULFILMENT OF THE REQUIREMENTS FOR THE

DEGREE OF MASTER OF SCIENCE

GRADUATE PROGRAM IN PSYCHOLOGY

CALGARY, ALBERTA

JULY, 2018

Abstract

The phenotypic role of activation transcription factor 4 (ATF4) in the mammalian circadian system has yet to be characterized. Previous research has provided evidence that ATF4 may play a key role in modulating molecular circadian activity, and it has been hypothesized that it may also be important for modulating photic resetting of the clock as a repressor of CREB. The main objectives of this investigation were to characterize the circadian expression of ATF4 protein in different lighting conditions, and to examine if downregulation of ATF4 using small interfering RNA (siRNA) technology would significantly potentiate photic phase shifts. In the Syrian hamster, ATF4 appeared to have a circadian expression in a light/dark cycle, but not when animals were in constant darkness. Light sufficiently increased ATF4 protein expression 2-3hrs following light exposure suggesting light plays an important role in regulating ATF4 expression. However, downregulation of ATF4 via siATF4 did not significantly potentiate phase advances to light as hypothesized. Rather, injections of siATF4 appeared to significantly alter an animal's phase angle of entrainment. In summary, ATF4 plays an important role in the rhythmicity of the clock as light appears to be important in driving ATF4 circadian expression and its downregulation resulted in increased phase angle. However, the function of light-induced ATF4 expression remains to be determined.

ACKNOWLEDGEMENTS

I wish to thank my supervisor and mentor, Dr. Michael Antle, for the opportunity to conduct research in his lab. His guidance, teachings, and insight have given me the necessary tools to be successful in research and gain a deep appreciation of the hard work and dedication required. I would also like to thank Dr. Victoria Smith and Dr. Glen Yamakawa, past members of the lab, for their patience and teaching me the necessary research skills during my undergraduate training. Lastly, thank you Dr. Simon Spanswick, Dr. Richelle Mychasiuk, and Dr. Jonathan Epp for serving on my defense committee.

DEDICATION

I wish to dedicate this work to my parents for their love, support, and hard work that have given me the opportunities that I have today. To my mom whose tenacity has shown me the importance of perseverance, and to my dad who has shown me the importance of balance. I would also like to dedicate this my partner in crime, Vanessa Wong, for always pushing me to become a better person and for the tremendous love, support, and encouragement that has allowed me to breakthrough the toughest of times. Lastly, I would like to dedicate this to my late grandma for all the little things and being a light in my life. For all the times you randomly made me snacks, for being my 5am breakfast companion after an overnight shift in the lab, and for all the quirky jokes and laughs. I love and miss you very much.

TABLE OF CONTENTS

LIST OF FIGURES

LIST OF ABBREVIATIONS

Measurement Terms:

°C	Degrees Celsius
hr(s)	Hour(s)
min	minutes
kg	kilogram
g	gram
mg	milligram
μg	microgram
L	liter
mL	milliliter
μL	microliter
M	Molar Concentration (mol/L)
mm	millimeter
µm	micrometer

Other Terms:

5-HT	serotonin, 5-hydroxytryptamine
5-HT_{1A}	5-hydroxytryptamine 1A receptor
ABC	avidin-biotin complex
AC	adenylyl Cyclase
AMPA	α-amino-3-hydroxy-5-methyl-4-isoxazolepropionic acid receptor
ANOVA	analysis of Variance
ApCREB	*Aplysia cAMP response-element binding protein* gene
ApCREB	Aplysia cAMP response-element binding protein
AP-1	activator protein-1
ATF4	activating transcription factor 4
bHLH	aasic helix-loop-helix
Bmal1	*Brain and Muscle ARNT-Like 1* Gene
BMAL1	Brain and Muscle ARNT-Like 1 Protein
bZIP	basic-region leucine zipper
CalB	calbindin
CamKII	Ca^{2+}-calmodulin dependent protein kinase II
cAMP	cyclic adenosine 3',5'-monophosphate
cDNA	complementary DNA
CK1δ, 1ε	casein kinase 1δ and 1ε
Clock	*Circadian Locomotor Output Cycles Kaput* gene
CLOCK	Circadian Locomotor Output Cycles Kaput protein
CRE	Ca2+/cAMP response element
CREB	cAMP response-element binding protein
Cry	*Cryptochrome* gene
CRY	Cryptochrome protein
CT	circadian time

DAB-IHC	diaminobenzidine immunohistochemistry
DD	constant darkness
DNA	deoxyribonucleic acid
ERK	extracellular signal-regulated kinase
FRP	free running period
GABA	gamma aminobutyric acid
GHT	geniculohypothalamic tract
GRP	gastrin-releasing peptide
IEG(s)	immediate-early gene(s)
IGL	intergeniculate leaflet
ipRGCs	intrinsically photosensitive retinal ganglion cells
LD	light/dark cycle
LTP	long-term potentiation
LP	light pulse
MAPK	mitogen-activated protein kinase
mRNA	messenger ribonucleic acid
mAtf4	mouse *Activating Transcription Factor 4* gene
NMDA	N-methyl-D-aspartic acid
NOS	nitric oxide synthase
NPY	neuropeptide Y
PACAP	pituitary adenylate cyclase-activated polypeptide
PAS	PER-ARNT-SIM
PBS	phosphate buffered saline
p-CREB	phosphorylated cAMP response-element binding protein
p-ERK	phosphorylated extracellular signal-regulated kinase
Per	*Period* gene
PER	Period protein
PKA	Protein Kinase A
PRC	phase response curve
RHT	retinohypothalamic tract
RORE(s)	retinoic acid-related orphan receptor (ROR)-binding element(s)
RyR	ryanodine receptors
SCN	suprachiasmatic nucleus
SP	substance-P
TTFL	transcription translation feedback loop
VIP	vasoactive intestinal polypeptide
VP	vasopressin
ZT	*zeitgeber* time

CHAPTER ONE: GENERAL INTRODUCTION

The suprachiasmatic nucleus (SCN) is the master mammalian circadian pacemaker that utilizes an increasingly complex web of transcription-translation feedback loops (TTFL) to drive endogenous rhythmicity and entrain to external cues termed *zeitgebers* (German for "time giver"). The predominant *zeitgeber* in mammals is light and it has the ability to alter the expression of clock genes in the SCN (Antle and Silver, 2005). Light input is received by the retinas and this photic signal is transduced into a secondary messenger cascade that activates cAMP-response element binding protein (CREB) at the level of the SCN (von Gall et al., 1998; Moriya et al., 2000). CREB increases the expression of *Period* genes, which are core components of the negative limb of the TTFL that drive circadian rhythmicity (Travnickova-Bendova et al., 2002; Tischkau et al., 2003). This altered expression of *Period* genes, *Per1* and *Per2*, is related to the phase resetting properties of light on circadian locomotor activity (Yan and Okamura, 2002; Yan and Silver, 2002, 2004). The objective of this investigation is to inquire about the potential role of activating transcription factor 4 (ATF4), a repressor of CREB transcription, in the circadian system and how its downregulation may potentiate photic phase shifts.

1.1 Rewinding the Clock - Circadian Fundamentals

1.1.1 Brief History of Circadian Rhythms

"Timing is everything". This colloquialism carries a heavy weight in the survival of organisms. Genetic fitness, the ability for a genotype to increase the probability of survival and reproduction, is greatly improved by the ability to predict temporal changes in the environment (Dunlap et al., 2004). Simply responding to exogenous cues (light, temperature, food availability, etc.) is not sufficient to be evolutionarily beneficial. Rather, an endogenous timekeeping mechanism allow organisms to optimally prepare physiological events and behaviours to account for these environmental changes. This manifests in forms of observable niches, such as diurnal vs nocturnal predators hunting at different times to decrease competition, or rodents foraging at night to minimize chances of predation. Rhythmic patterns of exogenous cues provide a scaffold for the internal clock to fine-tune its molecular gears to make the necessary adaptations.

The field of chronobiology focusses on understanding the internal timekeeping processes that are essentially exhibited by, and are necessary for, the survival of all organisms. There are various types of rhythms: circannual (period of about a year), circalunar (period of about a lunar cycle), ultradian (periods of less than a day), and circadian (period of about a day), to name a few. The focus of this study is on circadian (circa = "about", diem = "a day") rhythms to understand more about the molecular clocks that underlie timekeeping of about 24hrs. Circadian rhythms are a consequence of Earth's rotation with respect to the sun which generates periodic cycles of light and darkness over a 24hr period. Although not proven, it has been postulated that the molecular and cellular processes that underlie internal circadian rhythms occurs as an evolutionary response to cellular processes that are sensitive to UV radiation; processes more

sensitive UV radiation, such as DNA synthesis, occur during the night, while those less sensitive to UV radiation occur during the day (Pittendrigh, 1993). Others postulate that current time keeping molecules developed from similar ancient molecules sensitive to light resulting in the spontaneous generation of light-driven rhythms close to 24hrs (Edery, 2000). Through evolutionary processes, these ancient genetic gears have now developed into the timekeeping mechanism of modern day organisms; this is exemplified by the circadian bioluminescence of the eukaryotic *Gonyulax*, the circadian leaf movements of the *Mimosa pudica* plant, or perhaps more relevant to the current study, the wake-rest cycles of animals (Dunlap et al., 2004).

Although human interest in timekeeping is evident throughout history from the tracking of astronomical objects by ancient civilizations, the construction of Stonehenge, to the development of watches, the field of chronobiology is still relatively recent (Edery, 2000). Prior to the last 100 years, it has been generally believed that the cyclic nature of biological processes and behaviours were a consequence of exogenous rhythms (Dunlap et al., 2004). The first documented suggestion of an internal rhythm was by the French astronomer, Jean Jacques d'Ortous deMarian (1729), when he noticed that the daily opening and closing of leaf movements in the light sensitive *Mimosa pudica* plant could persist even in the absence of the light-dark (LD) cycles of the sun (Dunlap et al, 2004). However, it was not until Augustine de Condolle (1823), a Swiss Botanist, demonstrated that the *Mimosa pudica* had endogenously generated these circadian leaf movements in constant conditions with a free running period of 22-23hrs that more researchers began considering this paradigm shift of an endogenous timekeeping mechanism (Dunlap et al., 2004). In mammals, Maynard S. Johnson (1926 and 1939) recorded observations that the white-footed mouse, *Peromyscus leucopus*, had daily rhythmicity in locomotor activity even in constant darkness that persisted for months, while in

constant light this free-running period lengthened. Although these observations were accurate, the idea that biological entities had the ability to keep time in the absence of external cues was difficult for the scientific community to accept with the lack of evidence (Edery, 2000). Through the work of Colin S. Pittendrigh and Jürgen Aschoff, the pioneers of modern chronobiology who discovered and characterized many of the fundamental circadian properties, there was finally a general acceptance of an internal timekeeping mechanism and the multifaceted field of chronobiology began to flourish (Dunlap et al., 2004).

1.1.2 Entrainment and Desynchronization

Entrainment occurs when an organism's endogenous rhythm synchronizes, or more specifically matches phases with, an external rhythm. The predominant *zeitgeber* is light due to the natural consequence of the solar LD cycle. However, *zeitgebers* can also be non-photic such as circadian oscillations of temperature (important for certain cyanobacteria, fungi, and cold-blooded animals), food availability and exercise, and even social cues (eg. species-specific bird songs for social entrainment). However, non-photic *zeitgebers* are supplemental to light. This investigation will be focussed primarily on mammals and light as the principal *zeitgeber*.

In the absence of *zeitgebers*, organisms exhibit a free running rhythm, or free running period (FRP; or tau), which is representative of the clock's endogenous period. In rodents, this is typically measured non-invasively with graphical representations of daily wheel running activity (actograms). The rhythms of locomotor activity are highly representative of endogenous rhythmicity because it is robust and reliable; experiments have shown that rodents voluntarily seek out a running wheel, even if one is placed in the wild, and will begin to run almost immediately upon awaking (Dunlap et al., 2004; Meijer and Robbers, 2014). In the absence of an LD cycle, the concept of "day" and "night" are subjective. For nocturnal animals in constant

darkness, activity onset is denoted as CT12 (circadian time) and the active period is referred to as the animal's "subjective night", while its rest period would be referred to as its "subjective day". In an LD cycle, dark phase onset is denoted by ZT12 (*zeitgeber* time). The FRP can be easily determined by measuring the angle of the activity onsets for consecutive days. Mice typically have an FRP of ~23.5hrs, while hamsters are closer to ~24hrs (Weinert et al., 2001; Ripperger et al., 2011). In humans, the FRP is slightly longer at about ~24.1hrs, in which sex and ancestry have been found to play a significant role in its variance (Eastman et al., 2017). Although it is interesting to examine the FRP in constant conditions, the FRP is not truly an innate nor fixed property because the period changes depending on the type of constant conditions used as exemplified by Aschoff's Rule: increasing the light intensity in constant lighting conditions tends to lengthen the FRP of nocturnal animals, while decreasing the FRP in diurnal animals (Aschoff, 1951; Pittendrigh, 1960). More fascinating is how the internal circadian oscillator is fine-tuned with the ability to entrain and adjust to changes in light dark cycles.

1.1.3 Phase Response Curve (PRC) and Photic Phase Shifting/Resetting

Classically, there are two models of photic entrainment. Aschoff's *continuous* model suggests that varying light intensities exert continuous action on the clock to accelerate or decelerate the FRP according to the changes in the LD cycle. In contrast, Pittendrigh's *discrete* model proposes that the most important photic cues for entrainment occurred during dawn and dusk as they signify the beginning and end of the light phase. Since this investigation utilized Pittendrigh's *discrete* model, its intricacies will be further explored to explain the phenomenon of photic entrainment. When animals are free running in constant darkness, giving animals discrete light pulses that mimic dawn and dusk cues have the ability to shift or "reset" the phase of the endogenous oscillator (Pittendrigh, 1960). For a nocturnal rodent, a discrete light pulse

(LP) during the early subjective night (ie. “dusk” ends later) causes a phase delay in which the animal will wake up later in subsequent days while maintaining its FRP. Similarly, a LP in the late subjective night (ie. “dawn” beings earlier) results in a phase advance and the animal would wake up earlier in subsequent days. However, if a light pulse is given during the subjective day, there would be no shifts in the free running rhythm. Depending on LP duration, intensity, and timing with regards to the animal’s circadian phase, it can predict the magnitude and direction of the phase shift; this is described by the photic Phase Response Curve (PRC) (Figure 1.1; Pittendrigh, 1960). Although realistically these distinct periods of change in light intensity during dawn and dusk are gradual, the discrete model has high predictive value. Additionally, the PRC is species-specific and can be used for investigating non-photic *zeitgebers* as well.

How does the PRC explain the entrainment to LD cycles that have long phases of light input? For stable entrainment to occur in a LD cycle, the light signal needs to engage the PRC at a specific time point that allows for daily resetting of the clock (Dunlap et al., 2004). For example, if a nocturnal animal has a short FRP of 23hrs and needs to entrain to a 24hr LD cycle, there is a difference in period of 1 hr that needs to be accounted for by a daily phase shift (Phase shift = FRP – period of zeitgeber; Dunlap et al., 2004). The activity onset for this animal would occur approximately +1hr prior to dark phase onset; light exposure would occur during the delaying portion of its PRC profile resulting in daily phase delays of -1hr. The difference between activity onset and dark phase onset is known as the Phase Angle of Entrainment. Animals with longer FRPs would typically have a negative phase angle of entrainment adjusted by daily phase advances. These fundamental circadian properties have provided a non-invasive tool for countless researchers to analyze the effects of certain manipulations on the circadian system, which will also be crucial for understanding the analysis in this investigation.

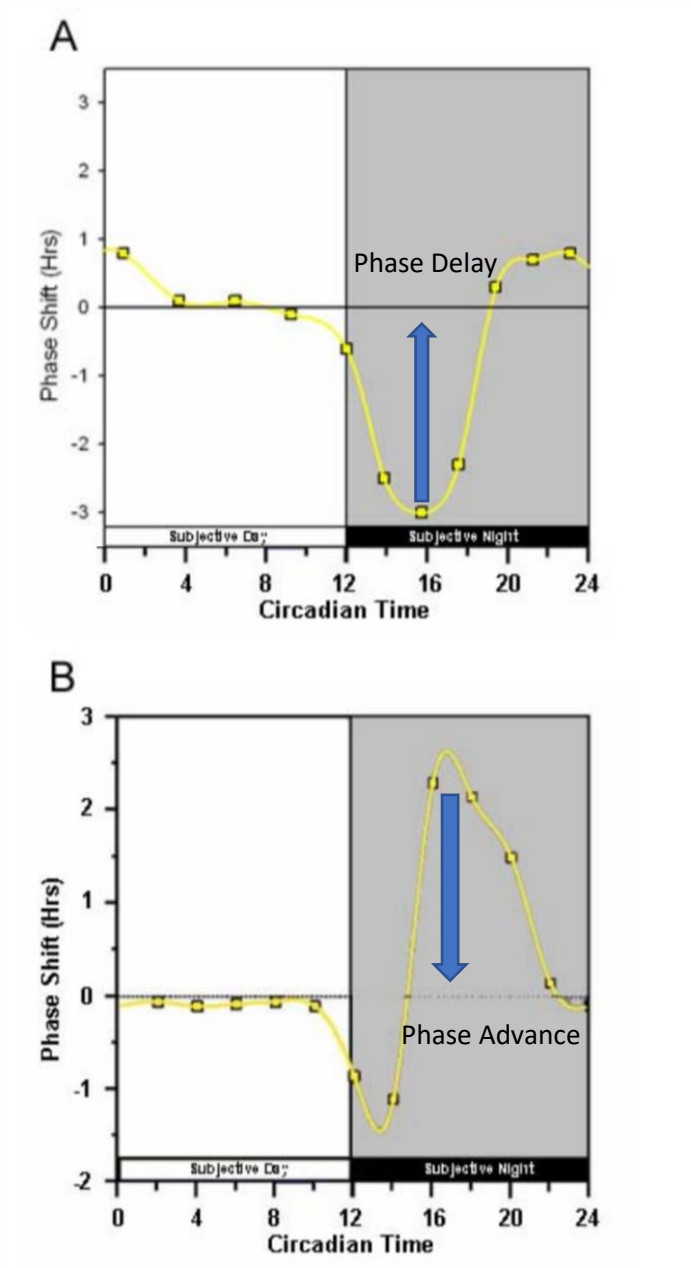

Figure 1.1. Examples of photic response curves of A) mice and B) hamsters. A) Mice typically have shorter free-running periods and exhibit stronger phase resetting to a light exposure during the early subjective night resulting in a phase delay. B) Hamsters typically have longer free-running periods and exhibit stronger phase resetting to light exposure during the late subjective night resulting in a phase advance.

1.2 The Suprachiasmatic Nucleus and its Molecular Gears

1.2.1 Discovery of the Master Mammalian Pacemaker

Most organs in the body exhibit autonomous circadian rhythmicity, but in the absence of input from the suprachiasmatic nucleus (SCN), the master mammalian pacemaker, their functions are not synchronized (Abe et al., 2002; Rosenwasser and Turek, 2015). The SCN consists of two nuclei with approximately 20,000 neurons, and it is situated in the anterior hypothalamus directly above optic chiasm (Reppert and Weaver, 2001). In 1880, the SCN was first characterized in a variety of metatherian and eutherian mammalian brains (Moore, 2013). However, indications that the SCN was the master pacemaker began in the 1970s when independent researchers interested in studying photic pathways and the neuroendocrine system observed that electrolytic lesions of the SCN resulted in the arrhythmicity of locomotor, adrenal corticosterone, and drinking behaviour rhythms (Richter, 1960; Moore and Eichler, 1972; Stephan and Zucker, 1972). These studies provided compelling evidence that the SCN was the location of the master clock, but huge variability was observed. To explain this variability, it was later discovered that if 20% of SCN neurons remained functional, rhythmicity could be sustained (Rusak, 1977). Despite the research indicating the SCN as the master clock, arguments were made suggesting that the SCN may play the role of a rhythmic integration system rather than generating its own rhythmic output (Weaver, 1998). Through the use of *in vivo* electrophysiology, it was demonstrated that if the SCN was surgically isolated in enucleated rats, rhythmic electrical activity in the SCN persisted but was lost in neighbouring SCN tissue; this critical experiment revealed the SCN to be an autonomous clock (Inouye and Kawamura, 1979). Remarkably, rhythmicity of adult SCN-ablated hamsters can be rescued through the implant of

fetal SCN tissue and even suspension of SCN cells highlighting the plastic nature of the SCN (Drucker-Colín et al., 1984; Sawaki et al., 1984; DeCoursey and Buggy, 1989; Silver et al., 1990). The discovery of the *Tau* mutant hamster (heterozygous period ~22hr, homozygous mutant period ~20hr) showed that SCN-ablated hamsters adopted the shortened period of the *Tau*-mutant SCN donor using this SCN transplantation (Ralph and Menaker, 1988; Ralph et al., 1990). After the indisputable establishment that the SCN is indeed the master mammalian pacemaker, research raced to characterize its network, cellular, and molecular properties.

1.2.2 SCN Morphology, Heterogeneity, and Afferent Pathways

Although the SCN is only a tiny bilateral nuclei of approximately 0.064mm^3 in volume, it has a variety of neuronal subtypes that are crucial for the generation of robust circadian rhythmicity and entrainment to exogenous cues (Moore, 2013). The rat SCN was originally characterized as a triaxial ellipsoid that spans dorsally along the optic chiasm with the dimensions about 360μm (dorsoventral), 450μm (mediolateral), and 750 μm (rostrocaudal) (Güldner, 1976; Van den Pol, 1980; Moore, 2013). SCN neurons can be classified into two major subpopulations: the rhythmic dorsomedial shell and the light-responsive ventrolateral core neurons (Antle and Silver, 2005). These subdivisions were first delineated with Golgi analysis and morphometry as researchers found more complex dendritic morphology and higher innervations from the retinohypothalamic tract (RHT) to the ventrolateral core (Van den Pol, 1980; Harrington et al., 1993).

Robust circadian rhythmicity in clock gene expression driven by a complex network of autoregulatory transcription-translation feedback loops (TTFL) is primarily confined to the dorsomedial shell region (Hamada et al., 2001, 2004; Yan and Okamura, 2002). Although individual neurons exhibit circadian rhythmicity in clock gene expression and electrical firing

activity (ie. high frequency firing during the day and low firing rate at night), they oscillate at varying phases or periods of 22-30hrs (Welsh et al., 1995; Herzog et al., 1998; Honma et al., 1998; Brown and Piggins, 2007). SCN coupling ensures that these neurons as a network remain synchronized to a common period to produce a robust circadian output (Herzog et al., 1998; Low-Zeddies and Takahashi, 2001). In contrast, ventrolateral core neurons do not exhibit the same rhythmicity in clock genes, but photic signals during the night increases SCN electrical activity and clock gene expression (Meijer et al., 1992; Hamada et al., 2001; Nakamura et al., 2004). Changes in clock gene expression due to light exposure occurs in core neurons before changes in shell neurons (Yan and Okamura, 2002; Yan and Silver, 2002). In abruptly changing LD cycle regimes (similar to traveling across time zones), the SCN core entrains to the new LD cycle quickly, while the SCN shell is slower to react with its activity resembling the previous LD cycle (Nagano et al., 2003; Nakamura, 2005). Although the precise mechanism is yet to be elucidated, the desynchrony between the core and shell gradually match phase through coupling (Mohawk and Takahashi, 2011). This highlights the importance of networking in the SCN to produce the emergent property of rhythmicity and the need to investigate the mechanism in which this coupling and communication occur.

SCN neurons are further classified into subpopulations based on neuropeptide expression. Effectively, all neurons in the SCN contain gamma-aminobutyric acid (GABA), which is colocalized with various neuropeptides (van den Pol and Tsujimoto, 1985; Moore et al., 2002). Although there are slight species differences, the SCN shell neurons primarily express vasopressin (VP), while core neurons express vasoactive intestinal polypeptide (VIP) and gastrin-releasing peptide (GRP) (Card and Moore, 1984; Mai et al., 1991; Moore et al., 2002; Antle and Silver, 2005). Additionally, hamsters also have further subpopulations of calbindin-

D_{28K} (CalB)-expressing cells and "cap" cells (i.e. light signals drive phosphorylated signal regulated kinase 1/2 rhythms; p-ERK) located in the ventrolateral core that colocalize with GRP-containing and VIP-containing cells (Silver et al., 1996; LeSauter et al., 2002; Lee et al., 2003). In addition to being useful immunolabeling tools, these neuropeptides are crucial in intraSCN communication between the two functional regions, especially in communicating photic information from core to shell (see section 1.2.4). Using immunocytochemistry and transynaptic transport assays, it has been demonstrated that axons of VP shell neurons form a complex web of innervation intrinsically and contralaterally with other shell neurons only; the retinorecipient VIP and GRP neurons send projections to the contralateral core and ipsilaterally to its respective shell counterpart (Card et al., 1981; Daikoku et al., 1992; Ibata et al., 1993, 1999; Moore, 2013).

The ventrolateral core is innervated by three main afferent connections. As previously discussed, both cores of the bilateral SCN receive photic information through direct retinal innervation by the RHT on to GRP, VIP, and CalB-containing neurons (Tanaka et al., 1997; Bryant et al., 2000). More specifically, intrinsically photosensitive retinal ganglion cells (ipRGCs) express the *Opn4* gene that produces melanopsin, which is the photopigment required for nonimage forming visual functions and circadian entrainment of the SCN (Provencio et al., 1998; Güler et al., 2008; Schmidt et al., 2011; Lucas et al., 2012). This was discovered when animals lacking rod and cone photoreceptors retained light-driven entrainment of locomotor rhythms and suppressed pineal melatonin release (Lucas et al., 2001). The second afferent pathway of the ventrolateral core is by the geniculohypothalamic tract (GHT). The optic nerve innervates the intergeniculate leaflet (IGL) that then projects to the SCN along the GHT that capable of phase shifting the clock through release of neuropeptide Y (NPY) (Morin, 1994; Harrington, 1997). Lastly, direct and indirect serotonergic projections from the median raphe

nuclei and dorsal raphe via the IGL innervate the SCN, respectively (Meyer-Bernstein' and Morin, 1996; Yamakawa and Antle, 2010). Endogenous serotonin has an inhibitory effect on photic signals reaching the ventrolateral core (Ying and Rusak, 1994; Rea and Pickard, 2000).

1.2.3 Transcription-Translation Feedback Loop

The cellular clock consists of various interconnected transcriptional autoregulatory feedback loops autonomously driven by clock genes that is not limited to only the SCN cells, but occur in most mammalian cells (Lowrey and Takahashi, 2011). With growing research, there continue to be additions to this molecular clock and our understanding of the intricacies of how it ticks improves (for a comprehensive review please refer to Lowrey and Takahashi, 2011; Takahashi, 2016). Many of these genetic gears are highly conserved throughout evolution, therefore many organisms share similar components. Specifically, in mammals, the positive limb of the core TTFL involves heterodimer of CLOCK (Circadian Locomotor Output Cycles Kaput) and BMAL1 (Brain and Muscle ARNT-Like Protein 1) proteins, which are repressed by the negative limb that consists of PER (Period) and CRY (Cryptochrome) proteins. CLOCK and BMAL1 are both basic helix-loop-helix (bHLH)- PER-ARNT-SIM (PAS) transcription factors that dimerize and bind to the E-Boxes (CACGTG) within the promoters of *per* (*per1*, *per2*, and *per3*) and *cry* (*cry1* and *cry2*) genes to increase their expression (King et al., 1997; Gekakis et al., 1998; Kume et al., 1999). As PER and CRY reach critical concentrations typically in late light phase, they form heterodimers that are translocated into the nucleus at night with the help of casein kinase 1δ (CK1δ) and CK1ε (Lee et al., 2001; Gallego and Virshup, 2007). PER-CRY bind to CLOCK-BMAL1 to inhibit their own transcription resulting in decreased PER and CRY levels. In the cytoplasm and nucleus, PER and CRY are targeted by specific E3 ubiquitin ligase complexes for degradation resulting in relatively short half-lives (Gallego and Virshup, 2007).

Following turnover of the negative limb, CLOCK-BMAL1 continue their activation of *Per* and *Cry* genes at the beginning of the next light phase.

CLOCK-BMAL1 also activate two other interconnected TTFLs involving: 1) REV-ERBα/β that compete with RORα/β/γ at the RevDR2 and retinoic acid-related orphan receptor (ROR)-binding elements (ROREs) of *Bmal1* promoter, and 2) PAR-bZip factors DBP (D-box binding protein) and NFIL3 (nuclear factor, interleukin-3 regulated protein) that compete at D-Box binding element of the Rora/Rorb promoter (Takahashi, 2016). Although these additional TTFLs will not be reviewed here, it highlights the importance of these cis-regulatory elements (E-Boxes, D-Boxes, and ROREs) not only in driving the cell-autonomous clock, but in driving the circadian control of specific clock output genes (Ueda et al., 2005).

1.2.4 Photic Pathway to the Circadian Clock

In mammals, when light is detected by the retina, photic information is received by ipRGCs containing melanopsin (Schmidt et al., 2011). This signal is transmitted down the unmyelinated monosynaptic RHT, which synapses onto the ventrolateral SCN core neurons (Moore and Lenn, 1972; Gooley et al., 2001). Glutamate and pituitary adenylate cyclase-activated polypeptide (PACAP: a member of the VIP, secretin, glucagon family) are released at the retinal terminals and exert their effects onto retinorecipient cells of the core. Glutamate binds to NMDA and AMPA receptors on core neurons causing membrane depolarization, removal of the NMDA Mg^{2+} block, and resulting in Ca^{2+} influx (Ding et al., 1994; von Gall et al., 1998; Moriya et al., 2000). Long term potentiation (LTP) in the SCN can be induced by tetanic stimulation of the optic nerve during the subjective day, which is followed by prolonged autophosphorylation of Ca^{2+}-calmodulin dependent protein kinase II (CamKII) in VIP neurons, exemplifying the synaptic plastic capabilities of the SCN (Nishikawa et al., 1995; Fukunaga et

al., 2002). PACAP acts as a co-transmitter and modulates the effects of glutamate in a concentration dependent manner and likely to be important for facilitating photic information during the daytime through the activation of presynaptic and postsynaptic adenylyl cyclase (AC)-protein kinase A (PKA) signalling pathway (Hannibal, 2006; Brown and Piggins, 2007). The increase in Ca^{2+} concentration is additionally enhanced by Ca^{2+} release from intracellular stores through ryanodine receptors (RyR) (Ding et al., 1998; Kim et al., 2005). Ca^{2+} activates a complex web of kinases including the activation of AC leading to the accumulation of cyclic adenosine 3',5'-monophosphate (cAMP) to activate PKA, activation of nitric oxide synthase (NOS), and CamKII that activates the mitogen-activated protein kinase (MAPK/ERK) pathway in a Ras-dependent manner (Obrietan et al., 1998; Butcher et al., 2002; Dziema and Obrietan, 2002; Lonze and Ginty, 2002; Schurov et al., 2002; Brown and Piggins, 2007). Ultimately, these pathways collectively phosphorylate ERK (p-ERK), which phosphorylates CRE-binding Protein (CREB) at the serine-133 and -142 sites to activate its transcriptional activities at the CRE promoters of its target genes in the nucleus (Ginty et al., 1993; Gau et al., 2002; Lonze and Ginty, 2002). Phosphorylated CREB (p-CREB) can bind to the CRE elements of immediate early genes (c-fos and JunB) and clock genes (*Per1* and *Per2*) to increase their gene expression (Rusak et al., 1992; Ginty et al., 1993; Shearman et al., 1997; Travnickova-Bendova et al., 2002; Tischkau et al., 2003).

Photic information received from the retinorecipient SCN core must be relayed to the rhythmic shell neurons for successful photic phase shifting and entrainment. Shell neurons typically have a shorter circadian period than the core, therefore coupling of the core with the shell is required for rhythmic precision (Noguchi et al., 2004). This is unidirectional as there are extensive projections from the core to the shell, but it is not reciprocated (Card and Moore, 1984;

Leak et al., 1999). The depolarization of core neurons by glutamate results in action potentials reaching the synaptic terminals targeting shell neurons, calcium influx, and the release of GABA, VIP, GRP, and substance-P (SP) (Antle and Silver, 2005; Welsh et al., 2010). These neuropeptides VIP, GRP, and SP bind to their respective receptors on the post synaptic shell neuron resulting again in elevated levels of Ca^{2+} and cAMP leading to the phosphorylation of CREB, increased *Per* and *Cry* expression, and ultimately phase shifting the period of the TTFL underlying circadian oscillations (Welsh et al., 2010). Experimental application of exogenous neuropeptides (VIP, GRP, and SP) onto the SCN are sufficient to induce photic-like phase shifts (Piggins et al., 1995; McArthur et al., 2000). These neuropeptides are highly colocalized and have compensatory photic resetting capabilities because only pharmacological inhibition of both GRP and VIP receptors results in attenuated photic phase shifts (Sterniczuk et al., 2010; Chan et al., 2016).

1.2.5 Light-Induced Gene Expression

CREB and its action on the CRE promoter is crucial for manipulating the molecular gears of the circadian clock. As previously stated, photic stimuli result in the increased expression of immediate early genes *c-fos* and *JunB* that dimerize to form activator protein-1 (AP1) binding complexes that result in further downstream transcriptional regulators (Rusak et al., 1992). SCN *c-fos* expression in the shell is rhythmic (peak during early day, low during the early night) and it is photic-inducible during the subjective night with expression levels correlated to the magnitude of the phase shift (Travnickova et al., 1996; Guido et al., 1999; Sumová and Illnerová, 2005). Additionally, the location of *c-fos* expression in the SCN changes depending on when a light pulse is given; light in the early subjective night increases *c-fos* expression primarily in the core, while a light pulse during the late subjective night increases *c-fos* expression in both the core and

shell (Rea, 1992). Although increased expression of IEGs do not directly affect the phase of the TTFL, *c-Fos* and *JunB* are important for photic phase shifting because antisense oligonucleotides that inhibit their expression effectively block phase shifts (Wollnik et al., 1995).

Photic-induction of CREB activity increases the expression of *Per1* and *Per2* in the SCN to directly reset the clock (Shearman et al., 1997b; Takumi et al., 1998; Maywood et al., 1999; Messager et al., 1999; Yan and Silver, 2002). The expression of *Per1* appears to be induced within 15-30min after a light pulse, while there appears to be an increased expression of *Per2* within 2hrs, both of which return to baseline after about 3hrs (Albrecht et al., 1997; Wilsbacher et al., 2002). Their expression also differs depending on when light exposure occurs during the subjective night; increased *Per1* expression is associated to photic phase advances, whereas increased *Per2* expression appears to be related to photic phase delays (Hamada et al., 2001; Yan and Silver, 2002). Specifically in the rhythmic shell region, during the early subjective night (phase delaying light pulse) when levels of PER protein are falling, light increases the expression of both *Per1* and *Per2* (Yan and Silver, 2004). However, when PER protein levels are rising during the late subjective night (phase advancing light pulse), light exposure only increases *Per1* further, but not *Per2* (Yan and Silver, 2004). In addition to the temporal specificity of photic-induction, there are spatial differences between *Per1* and *Per2* expression. After a phase delaying light pulse, *Per1* is localized primarily in the retinorecipient GRP cells, while *Per2* expression is more wide-spread and is expressed in both the core neuronal population and VP cells of the rhythmic shell (Dardente et al., 2002). Additionally, a phase advancing light pulse increases *Per1* expression in CalB core neurons within one hour after a light pulse, which is followed by increased *Per1* expression in the shell within the following 30 min. (Hamada et al., 2004). The altered expression of clock gene expression due to light demonstrates the importance

of the CRE promoter as a crucial component in regulating the circadian response to light. It would be important to research molecular components that modulate CREB activity in the SCN and how they may affect the photic resetting of the clock.

1.3 Considerations from Circadian Serotonin Experiments

1.3.1 Endogenous Serotonin in the Circadian System

As previously mentioned, the ventrolateral SCN core is also densely innervated by serotonergic fibers directly from the median raphe nucleus and indirectly from the dorsal raphe nucleus (Meyer-Bernstein' and Morin, 1996; Pickard and Rea, 1997; Yamakawa and Antle, 2010). This places endogenous serotonin (5-hydroxytryptamine; 5-HT) in an opportune position to participate not only in non-photic phase resetting of the clock, but also to modulate photic responses. Serotonin has a variety of functions on the SCN due to the numerous receptor subtypes; however, with regards to its modulation of photic effects, it acts as an inhibitory neurotransmitter by reducing light-induced excitation of core neurons (Meyer-Bernstein' and Morin, 1996; Jiang et al., 2000). At the beginning of the subjective night, there is a sharp increase in 5-HT release that returns to baseline over time (Dudley et al., 1998). Electrically stimulating the median raphe to increase the release of 5-HT onto the SCN reduces its firing rate, and ablation of this pathway potentiates photic phase advances, increases FRP, and reduces entrainment time (Pickard and Rea, 1997).

1.3.2 Manipulation of Serotoninergic Effects on Photic Phase Shifts

A variety of pharmacological manipulations have been used to investigate how the serotonergic system modulates the photic input to the SCN. Due to the large variation of 5-HT receptor subtypes found in the SCN (5-HT_{1A}, 5-HT_{1B}, 5-HT_{2A}, $5HT_{2C}$, 5-HT_{5A}, and 5-HT_{7}) and lack of specificity in many of these pharmacological agents, researching the precise role of serotonin has been difficult and contradictory (Ying and Rusak, 1994; Smith et al., 2001; Niesler et al., 2007). This discussion will focus mainly on the 5-HT_{1A} receptor as it appears particularly important in regulating circadian responses to light (Smith et al., 2008, 2015a). 8-OH-DPAT, a 5-HT_{1A} receptor agonist, attenuates behavioural photic phase shifts when injected systemically or intracranially, as well as inhibiting light-induced *c-fos* expression in the SCN (Rea et al., 1994; Rea and Pickard, 2000). Antagonism of the 5-HT_{1A} receptor with WAY-100635 enhances photic phase shifts (Rea et al., 1995; Smart and Biello, 2001). However, these results have been complicated by species dependent differences (Rea et al., 1994; Kennaway et al., 1996; Recio et al., 1996; Antle et al., 2003).

Of particular interest are serotonergic mixed agonists/antagonists that act as antagonists on postsynaptic 5-HT_{1A} receptors of targeted core neurons, and agonists on 5-HT_{1A} somatodendritic autoreceptors of the presynaptic neuron from the raphe (Gannon, 2003). It has been hypothesized that antagonism of the postsynaptic receptors will remove the inhibition of serotonin on the SCN core, while the autoreceptors decrease 5-HT secretion from the presynaptic raphe neurons resulting in further loss of serotonergic inhibition of light-induced signaling to the ventrolateral core (Gannon, 2003; Gannon and Millan, 2006). Typically, when a dim light pulse is presented to an animal during its late subjective night, it causes phase advances in its locomotor activity of about two hours that require a few days to transition and stabilize.

However, systemic application of mixed 5-HT agonists/antagonists, NAN-190 and BMY7378, potentiates this effect by about three times (~6hrs) while reducing transience period (Byku and Gannon, 2000; Lall and Harrington, 2006). This effect is still observed even when these drugs are administered systematically 6 hours after a light pulse (Kessler et al., 2008; Lungwitz and Gannon, 2009). Therefore, mixed 5-HT agonists/antagonists may be affecting the intracellular pathways downstream at the level of transcription and translation (Kessler et al., 2008).

Increased phosphorylation of CREB leading to increased *c-fos* expression has been typically correlated with larger phase shifts (Kornhauser et al., 1990). However, pre-treatment with NAN-190 actually decreases expression of light-induced *c-Fos* and phosphorylation of CREB (Recio et al., 1996; Smith et al., 2010). More recent evidence suggests that BMY7378 systemic injection also does not increase light-induced c-Fos protein expression for the first 120min following a phase advancing light pulse, but does produce a significant increase in the number of c-Fos, as well as JunB and PER1, expressing cells at 360min following a light pulse (Smith et al., 2015b). This corresponded with potentiated photic phase advances. Additionally, the number of p-ERK and p-CREB expressing cells does not vary significantly within 120min of light exposure (Smith et al., 2015b). This provided further evidence that these drugs may be exerting their effects upstream of the induction of IEGs and clock genes without affecting the level of phosphorylation of ERK and CREB. It was hypothesized that these drugs may be exerting their potentiating effect by disrupting the termination CRE-mediated transcription required by *c-Fos*, *JunB*, and *Per1* genes. This hypothesis presents a plausible reason to explain how these drugs can potentiate phase advances even when injected after light exposure. This investigation aimed to examine activation transcription factor 4 (ATF4) as a potential the "brake" in CRE-mediated transcription in the SCN.

1.4 ATF4 and Circadian Rhythms

1.4.1 Overview of ATF4

Activation Transcription Factor 4 (ATF4/CREB2) is classified as a member of the activated transcription factor (ATF)/cAMP response element binding protein (CREB) family and is involved in numerous signaling pathways involving osteogenesis, eye development, cancer drug resistance, apoptosis, and modulation of metabolic stress, but its role in the circadian system is not well established (Hai and Curran, 1991; Ameri and Harris, 2008). Due to its multitude of functions, ATF4 knock-out mice are frail with decreased bone mass, blind, anaemic, and subfertile (Ameri and Harris, 2008). This ATF/CREB family of proteins all contain a basic-region leucine zipper (bZIP) domain with the ability to bind to the TGACGT(C/A)(G/A) consensus sequence, which is identical to the CRE promoter (TGACGTCA) (Deutsch et al., 1988; Lin and Green, 1988). Nomenclature of the ATF4 has been confusing because its cDNA has been cloned and isolated by various research groups in various species under differing names (ie. human ATF4 as TAXCREB67 and CREB2, or mouse ATF4 as mATF4, mTR67, and C/ATF), but it is collectively referred to as ATF4 because members in this subclass share 55% similarity to mouse mATF4 (Mielnicki and Pruitt, 1991; Tsujimoto et al., 1991; Chevray and Nathans, 1992; Karpinski et al., 1992; Vallejo et al., 1993; Hai and Hartman, 2001). The ATF4 gene can be found on chromosome 22 in human and chromosome 15 in mice, but the chromosome location has yet to be determine for Syrian hamsters (*Mesocricetus auratus*) although its protein and cDNA sequence has been identified (Ameri and Harris, 2008; McCann et al., 2017). ATF4 mRNA is ubiquitously expressed, while its protein is present at low levels with a short half-life of 30-60 min (Vallejo et al., 1993). The ATF4 protein consists of 351 amino

acids that contain various domains/motifs crucial for its complex interactions with other proteins and binding to the CRE promoter (Ameri and Harris, 2008). For example, $SCF^{\beta TrCP}$ class of ubiquitin ligase signals ATF4 for proteasomal degradation through phosphorylation at its βTrCP recognition motif (DSGXX(X)S), while histone acetyltransferase p300 (HAT p300) inhibits this degradation through acetylation at the N-terminal (Lassot et al., 2001, 2005). Additionally, the bZIP motif at the C-terminal of ATF4 not only allows binding to CRE promotors but also the formation of homodimers and heterodimers with members of the AP-1 and C/EBP family of proteins including Fos and Jun (Hai and Curran, 1991; Chevray and Nathans, 1992; Karpinski et al., 1992). Based on cellular and molecular context, ATF4 functions both as a transcriptional activator and repressor; only the repressor activity of ATF4 will be reviewed and examined in the context of circadian rhythms.

1.4.2 Potential Role of ATF4 a Member of the TTFL

Initial indications that suggested ATF4 as a crucial player in the circadian system arose from the study of cancer resistant drugs (Igarashi et al., 2007). They showed that the *Atf4* gene was a direct target of CLOCK via the E-Box element in the *Atf4* promoter *in vitro* (Igarashi et al., 2007). Further studies in mice show that *mAtf4* exhibits significant circadian oscillations in the liver, kidney, cerebral cortex, and SCN with its peak during the light phase (~ZT6) followed by a decrease during the dark phase (Koyanagi et al., 2011). In further support of *Atf4* as a direct target of CLOCK, Koyanagi et al. (2011) show that *Clock/Clock* double knockout mutant mice, when compared to wild-type mice, did not exhibit *mAtf4* circadian rhythmicity. Additionally, ATF4 significantly bound to the CRE element of the *Per2* gene and appears to be a stronger circadian regulator when compared to the traditional E-Box and CLOCK-BMAL1 interaction (Koyanagi et al., 2011). This was shown *in vitro* by using a mutated CRE *Per2* promoter to

abolish Per2::Luc bioluminescence despite having an intact E-Box and regular circadian oscillations of CLOCK and BMAL1 (Koyanagi et al., 2011). CREB preferentially binds to the CRE within the *Per1* promoter, while ATF4 preferentially binds to the CRE within the *Per2* promoter (Travnickova-Bendova et al., 2002; Koyanagi et al., 2011). These studies set the stage for ATF4 to potentially have an intermediate role in the genetic orchestra of molecular clocks as a target of CLOCK and regulator of PER2.

1.4.3 Potential Role of ATF4 in Photic Phase Resetting as a Repressor of CREB

Traditionally, ATF4/CREB2 has been demonstrated to be a repressor of CRE-dependent gene transcription specifically for long-term memory storage (Bartsch et al., 1995; Chen et al., 2003). In *Aplysia,* ApCREB1 and ApCREB2 have been hypothesized to form positive and negative feedback loops with each other using both canonical and variant CRE motifs (Mohamed et al., 2005). With the administration of serotonin (5-HT) in *Aplysia*, ApCREB1 is phosphorylated by protein kinase A (PKA) intracellular pathways leading to the binding of the canonical CRE element of its own promoter region and the variant CRE of the *ApCreb2* promoter region to activate the transcription of both (Bartsch et al., 1995, 1998; Mohamed et al., 2005). Firstly, this indicates that p-CREB creates a positive feedback loop by enhancing its own transcription (Mohamed et al., 2005). Secondly, there are gene-specific CRE motifs that preferentially bind to the CREB proteins (Mohamed et al., 2005). The negative feedback loop occurs when ApCREB1 enhances the transcription of ApCREB2, which competitively binds to the variant CRE motif of both its own gene and the *ApCreb1* gene to hinder the progression of RNA polymerase II, ultimately repressing the expression of *ApCreb1* and itself (Hai and Hartman, 2001; Mohamed et al., 2005). *In vivo* single application of 5-HT application normally results in short-term facilitation that decays over 10 minutes (Bartsch et al., 1995). However, if

5-HT application is followed by the disinhibition of the ApCREB1 promoter using anti-ApCREB2 antibody, the induction of long-term facilitation occurs; a requirement of long term synaptic plasticity and memory formation (Bartsch et al., 1995). Although caution is advised when interpreting the translational effect of serotonin directly on CREB and ATF4 activity in mammals due to the various serotonin receptor subtypes, especially in the SCN, it provides evidence to support the potential role of ATF4 in modulating the effects of light-induced CREB activity in the SCN.

1.5 Research Objectives

Previous research suggests that ATF4 may be a potential candidate to be a "brake" in light-induced CREB activity in the SCN and photic phase resetting. The activity of 5-HT mixed agonist/antagonists function to decrease this inhibitory serotonergic activity on photic induction of the retinorecipient ventrolateral SCN core (Gannon, 2003; Gannon and Millan, 2006). Despite systemically administering these drugs before or after a light pulse, significant potentiation of phase advances are still observed in hamsters (Byku and Gannon, 2000; Lall and Harrington, 2006). Investigation of *c-fos, JunB,* and *Per1* downstream of the photic pathway suggest that 5-HT mixed agonist/antagonists may be prolonging their increased expression to light, without significantly altering levels of p-ERK and p-CREB (Recio et al., 1996; Smith et al. 2010, 2015b). Investigating the cause of this phenomenon would expand our knowledge of how the molecular clock regulates photic-information and perhaps provide further insight into the limits of entrainment.

Investigation into the circadian importance of ATF4 has been lacking. This investigation was the first to investigate the role of ATF4 in the circadian system *in vivo*. It had three primary objectives: 1) to examine if ATF4 proteins exhibit circadian expression in Syrian hamsters in LD and in DD, 2) to characterize the effect of light exposure during the late subjective night on ATF4 expression, and 3) to examine if downregulation of ATF4 expression in the SCN using small interfering RNA (siRNA) technology can potentiate photic phase shifts. It was hypothesized that ATF4 exhibits rhythmic expression and its expression is induced by light as a response to repress CREB activity along the photic pathway. Furthermore, suppression of ATF4 using siRNAs was hypothesized to potentiate phase shifts to light through the disinhibition of CREB-driven transcription of downstream IEGs and clock genes to prolong their expression.

CHAPTER TWO: CIRCADIAN ATF4 EXPRESSION IN THE SCN

2.1 Introduction

It has been postulated that ATF4 may play an important role in the circadian system. *Atf4* appears inducible by CLOCK, while the ATF4 protein regulates Per2 expression at its CRE promoter (Igarashi et al., 2007; Koyanagi et al., 2011). It was even suggested to be a stronger regulator of the negative limb of the TTFL than the traditional action of CLOCK-BMAL1 at the E-Box promoter of *Per2* (Igarashi et al., 2007; Koyanagi et al., 2011). Additionally, *mAtf4* in the SCN of mice has peak expression during the light phase (~ZT6) with significantly lower expression during the dark phase (~ZT18) (Koyanagi et al., 2011). However, these studies utilized QT-PCR to quantify its mRNA circadian expression of the SCN. This lacked spatial information as well as information on protein circadian expression. Since ATF4 has a short half-life of 30-60 min, it was hypothesized that its protein expression should follow a similar circadian profile as its mRNA expression (Experiment 1; Vallejo et al., 1993). Furthermore, previous research has only explored *mAtf4* expression in an LD cycle (Koyanagi et al., 2011). If ATF4 is a stronger driver of the clock than the more traditional members of CLOCK-BMAL1, ATF4 would be expected to also exhibit a significant circadian expression in constant darkness (Experiment 2). However, if ATF4 does not display a significant circadian expression profile in constant darkness, it may be light-dependent and therefore light-inducible. Previous research has indicated that increased activation of CREB leads to the increased expression of CREB2 (homolog of ATF4) to repress CREB transcription (Mohamed et al., 2005). Since light exposure quickly leads to increased CREB expression and activation in the SCN, it was hypothesized that ATF4 will also have increased expression soon after light exposure to limit and suppress the expression of CREB (Experiment 3; Ginty et al., 1993; Lonze and Ginty, 2002). It was

hypothesized that animals in constant darkness will show increased ATF4 expression about 2-3 hours following light pulse at CT18.

The primary objectives of these experiments were to provide insight to three major questions: 1) is there circadian expression of ATF4 in the Syrian hamster SCN while in a LD cycle, 2) could this circadian expression be observed in the absence of light, and 3) would a brief light exposure be sufficient in enhancing ATF4 expression in the SCN 2-3 hours after?

2.2 Materials and Methods

2.2.1 Animals and Housing

This experiment used a total of 59 male Syrian Hamsters (*Mesocricetus auratus*, 110-180g). Eleven animals were utilized in the pilot studies. Hamsters were supplied either from the Charles Rivers Labs (Kingston, NY) or through the ongoing breeding program in the lab. Animals arriving in the lab were given one week to acclimatize to the new environment, while in house bred animals were required to reach the minimal weight prior to experimentation. Initially, animals were pair housed in polycarbonate cages (22x45x22 cm) at room temperature (21°C) in a 14:10 light-dark (LD) cycle with a cage level illuminance of approximately 300 lux. Cages were changed bi-weekly, while food and water were provided ad libitum. Handling of animals in complete darkness during the experiment was done with the assistance of night vision goggles (BG15, Alista, Richmond Hill, Ontario, Canada). All protocols were approved by the University of Calgary Life and Environmental Sciences Animal Care committee and adhered to the Canadian Council Animal Care guidelines.

2.2.2 Activity Rhythms

To track circadian rhythms in locomotor activity, hamsters were provided with running wheels equipped with magnetic switches that were activated by wheel revolution. Graphical records of wheel running activity (actograms) were collected continuously using Clocklab Data Collection software (Coulbourn Instruments Allentown, PA). Using the Clocklab Analysis software, regression lines were fitted to a minimum of seven days of stable activity onsets for making predictions of the following activity onset. Activity onset represents an animal's CT12 and was defined by the software as the first hour of activity bins that exceeded the 50^{th} percentile of average activity after 5 hours of activity below the 50^{th} percentile.

2.2.3 Immunohistochemistry

Hamsters were deeply anesthetized using 0.4mL of sodium pentobarbital (Euthanyl, MTC Pharmaceuticals, Cambridge, ON, Canada). They were first perfused intracardially with ~100mL of cold phosphate buffered saline (PBS) followed by ~100mL of 4% paraformaldehyde to fix the tissue. Brains were removed and placed in 4% paraformaldehyde solution for another ~18-24hrs to allow for further fixation. Brains were then cryoprotected in a 20% sucrose solution at 4°C for a minimum of 48 hours.

The diaminobenzidine (DAB)- immunohistochemistry (IHC) protocol used was based on previous studies from our laboratory (Antle et al., 2008). Unless otherwise specified, all rinses were done on a shaker tray at room temperature. Alternating brain sections were sliced and collected at 35μm using a Leica Cyrostat at -18°C and were placed in plastic/nylon wells filled with phosphate buffered saline (PBS). To inactivate endogenous peroxidases, sections were rinsed for 15min in 0.5% H_2O_2 in PBSx (PBS with 0.3% Triton X-100) and then rinsed three times with PBSx for 10min each. Afterwards, slices were incubated in 5% normal goat serum in

PBSx for 90min followed by a 48hr incubation at 4°C in the primary antibody for ATF4 (rabbit anti-ATF4 (human); PA5-19521; Invitrogen). Concentration of the primary antibody varied among the experiments: experiment 1 = 1:4000, experiment 2 = 1:1000, and experiment 3 = 1:250. The initial set of primary antibody used in experiment 1 produced a robust signal, while the signal of the second batch of primary antibody used in experiment 2 and 3 was not as robust, which explains the increased concentration used. Tissue slices were then subjected to three 10min rinses with PBSx, 1hr incubation in the secondary antibody biotinylated goat anti-rabbit (1:200; Vector Laboratories, Burlingame, CA, USA), three more 10 min PBSx rinses, a 1hr incubation in ABC (Vectastain Elite kit, Vector Laboratories, Burlingame, CA, USA), and another 10min PBSx rinses. For approximately 15-45min, slices were developed in 24mL of 0.1M Tris buffer, 0.05% DAB, and 0.02% NiCl solution that was activated by 80μL of 30% H_2O_2. Slices were mounted on to gelatin-coated slides, air-dried for at least 1hr, dehydrated through an alcohol series, cleared with xylenes, and cover slipped with Permount (Fisher Scientific, Pittsburgh, PA, USA).

2.2.4 Quantification of ATF4 Expression

Images of the DAB stained brain tissue were captured using a 20x objective on an Olympus BX51 microscope equipped with a QICam Fast 1394 digital video camera (QImaging, Burnaby, BC, Canada). ATF4 expression was analyzed by the manual cell counting function on ImageJ 1.34s (National Institutes of Health, Bethesda, MD, USA). One representative slice of the central caudal SCN, determined by anatomical shape and tissue integrity, from each animal was selected for analysis of cellular ATF4 protein expression. The coronal slices of the central-caudal SCN were selected because it contained both the dorsomedial shell and the ventrolateral core neuronal populations of the SCN (Card and Moore, 1984). To standardize counting area, an

elliptical shape (width=200µm, height=250µm) was used as the boundary for the manual cell counting.

2.2.5 Experiment 1 Procedure – ZT expression of ATF4

Hamsters (n=12) were given running wheels and placed in a 14:10 LD cycle (lights off at ZT 12, lights on at ZT22) for at least seven days prior to experimentation. Activity onsets were monitored to ensure stable entrainment. A total of 12 hamsters were used and were perfused at four different time points following entrainment: ZT6 (n=3), ZT12 (n=3), ZT18 (n=3), and ZT24 (n=3). After the animals were deeply anesthetized using Euthanyl, their heads were wrapped with tin foil to prevent an effects of light stimulus during the perfusion process. Brain tissue collection and DAB-IHC (primary ATF4 antibody concentration = 1:4000) was used to examine ATF4 expression in the SCN. A one-way analysis of variance (ANOVA) was used to determine if there was a significant difference in the number of ATF4 expressing cells in the SCN across the different time points. A significant ANOVA was followed by a post-hoc multiple comparisons using Tukey's Test.

2.2.6 Experiment 2 Procedure – CT Expression of ATF4

In contrast to Experiment 1, hamsters (n=24) were given running wheels and placed in constant darkness for seven days to obtain a stable free running period (FRP). Utilizing the activity onsets of an animal's FRP, CT12 was predicted for the following day and animals were perfused at four different time points according to the animal's individual FRP: CT6 (n=3), CT12 (n=3), CT18 (n=3), and CT24 (n=3). Brain tissue was collected in a similar manner to experiment 1, but the batch of ATF4 primary antibody used had a less robust signal, therefore a concentration of 1:1000 was used. This resulted in the loss of data from the initial set of 12 animals at 1:4000. Again, a one-way ANOVA was used to analyze if there was a significant

difference in the number of ATF4 expressing cells in the SCN across the different time points. A significant ANOVA was followed by a post-hoc multiple comparisons using Tukey's Test.

2.6.7 Experiment 3 Procedure – Light-Induced Expression of ATF4

Similar to experiment 2, hamsters (n=12) were placed in DD for 7 days prior to manipulation. Some animals were given a bright light pulse (~300 lux) for 15 min by placing the individual animals in the well-lit lab space at CT18, while the others (n=6) remained in the dark room during CT18. Following the LP, animals were either perfused at CT20 (2 hours later) or CT21 (3 hours later). These time points were used because it was hypothesized to be when light-induced CREB would increase the expression of its repressor, ATF4. Collectively, there were four conditions: 1) CT20 (n=3), 2) CT20+LP (n=3), 3) CT21 (n=3), and 4) CT21+LP (n=3). Brain tissue was obtained and DAB-IHC was used to examine ATF4 expression in the SCN. Since DAB signal still appeared weak at 1:1000 using the second batch of primary antibody in experiment 2, the antibody concentration was increased to 1:250 for this experiment. A between-subjects two-way ANOVA was used to determine if brief light exposure would significantly increase the number of ATF4 expressing cells in the SCN at CT20 and CT21. A significant ANOVA was followed by a post-hoc multiple comparisons using Tukey's Test.

2.3 Results

2.3.1 Experiment 1 – ZT expression of ATF4

DAB-IHC was performed on hamsters (n=12) perfused at four time points during a 14:10 LD cycle (Figure 2.1A). Manual cell counts were done on unilateral representative caudal SCN sections and quantified by a one-way ANOVA. There was a significant difference of *zeitgeber* time on the number of ATF4 expressing cells in the SCN (Figure 2.2A; $F_{3,8}$=7.817, p=.009). More specifically, SCN slices at ZT18 (M=206.67, SEM=39.73) had significantly less ATF4 expressing cells when compared to ZT6 (M=410.33, SEM=38.61; p=.036) and ZT24 (M=484.33, SEM=8.99; p=.007), but not when compared to ZT12 (M=360.67, SEM=62.52).

2.3.2 Experiment 2 – CT Expression of ATF4

DAB-IHC was performed on hamsters (n=12) perfused at four time points along their circadian time during constant darkness (Figure 2.1B). Similar to experiment 1, manual cell counts were performed on representative SCN sections and quantified by a one-way ANOVA. There were no significant differences of circadian time on the number of ATF4 expression cells in the SCN (Figure 2.2B; $F_{3,8}$=3.690, p=.062). The time points CT6 (M=518.67, SEM=43.39), CT12 (M=656.00, SEM=17.78), CT18 (M=486.50, SEM=46.72), and CT24 (M=558.00, SEM=51.05) did not significantly differ from one another.

Figure 2.1. Representative coronal sections of the mid-caudal SCN exemplifying ATF4 protein expression of hamsters in a 14:10 LD cycle (A) or constant darkness (DD) (B). ZT12 indicates beginning of dark phase onset, while CT12 represents activity onset. Brain tissue was collected in 6-hour intervals. OX = optic chiasm, 3V = third ventricle, and the scale bar = 200μm.

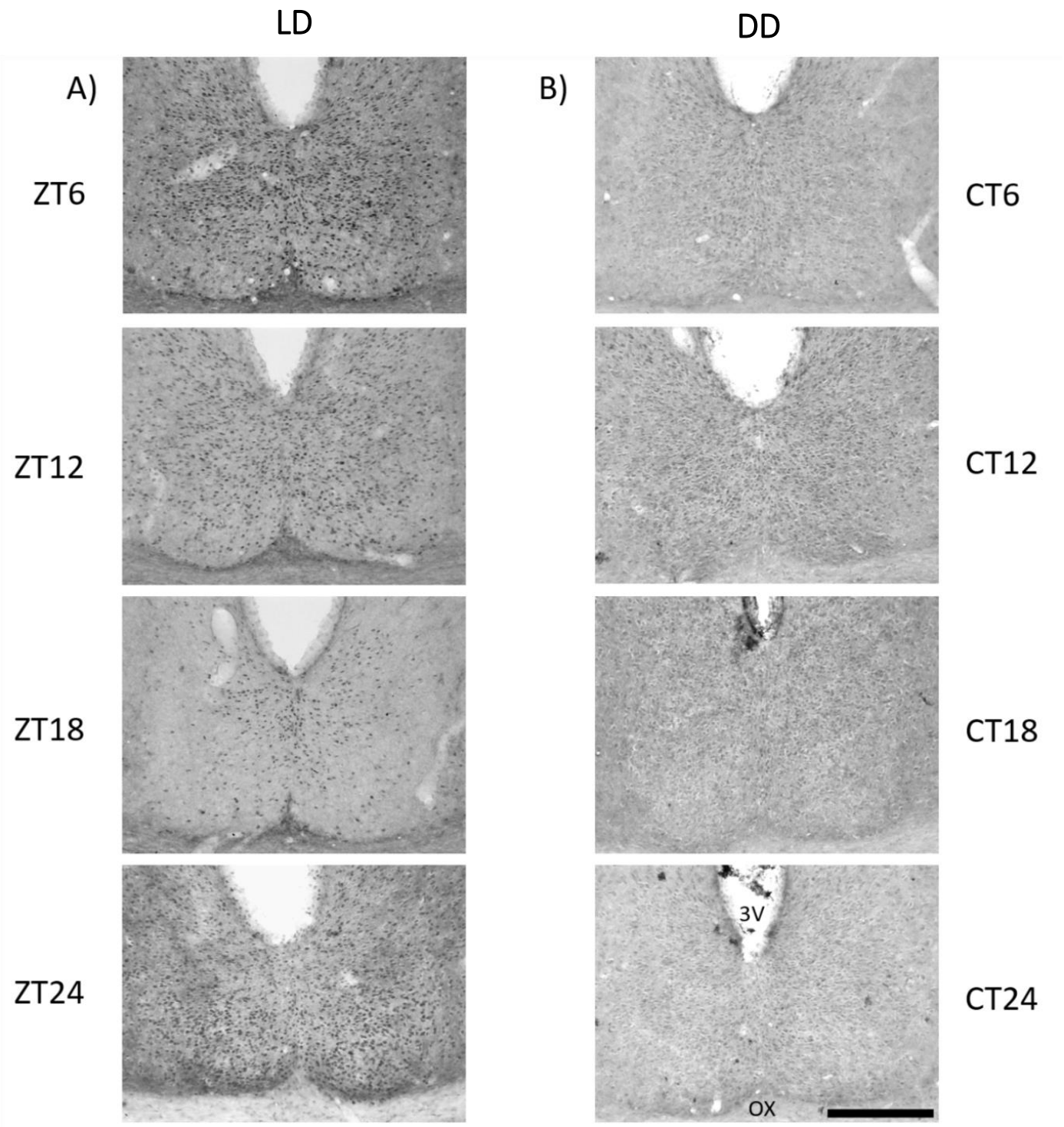
LD
DD
A)
B)
ZT6
CT6
ZT12
CT12
ZT18
CT18
ZT24
CT24
3V
OX

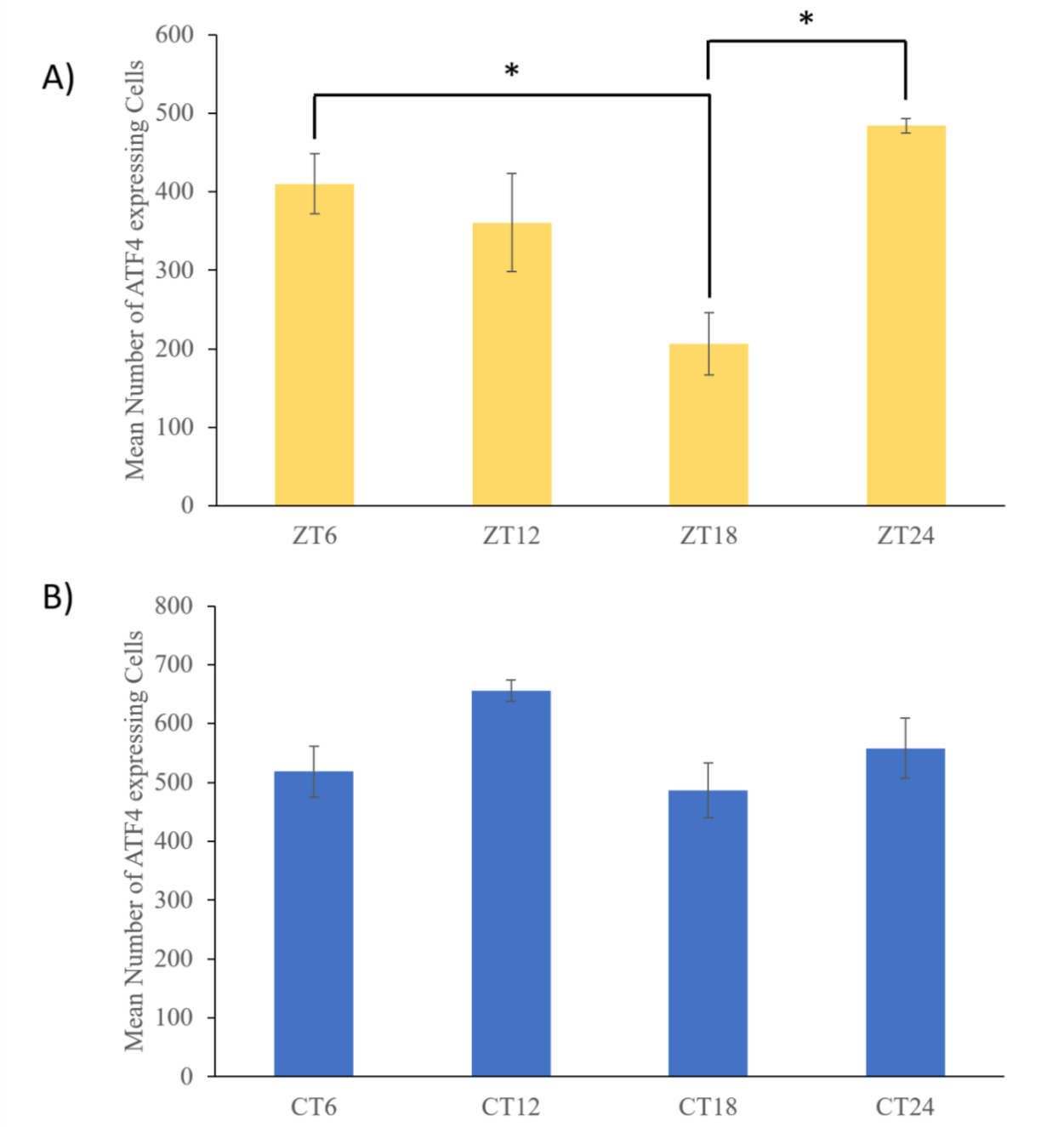

Figure 2.2. Mean manual cell count of the number of ATF4 protein expressing cells from hamsters housed in a 14:10 LD cycle (A) and in constant darkness (B). Statistical significance of $p<.05$ was denoted by (*). Error bars represent ± SEM.

2.3.3 Experiment 3 – Light Induced Expression of ATF4

To determine if brief light exposure was sufficient to induce an increase in the number of ATF4 expressing cells in the SCN, DAB-IHC was performed on hamsters (n=12) at CT20 or CT21 after no light pulse or a light pulse at CT18 (Figure 2.3). A 2x2 between-subjects ANOVA was used to analyze the data. There was no significant interaction between CT time and light manipulation on the number of ATF4 expressing cells ($F_{1,8}$=.104, p=.755; Figure 2.4). Additionally, there was no significant main effect of CT time on ATF4 expression ($F_{1,8}$=.384, p=.553). However, there was a significant main effect of light manipulation on the number of ATF4 expressing cells ($F_{1,8}$=16.579, p=.004), therefore exposure to a brief light pulse (M=653.17, SEM=15.21) significantly increased the number of ATF4 expressing cells, averaged over CT20 and CT21, when compared to no light pulse (M=525.00, SEM=24.69).

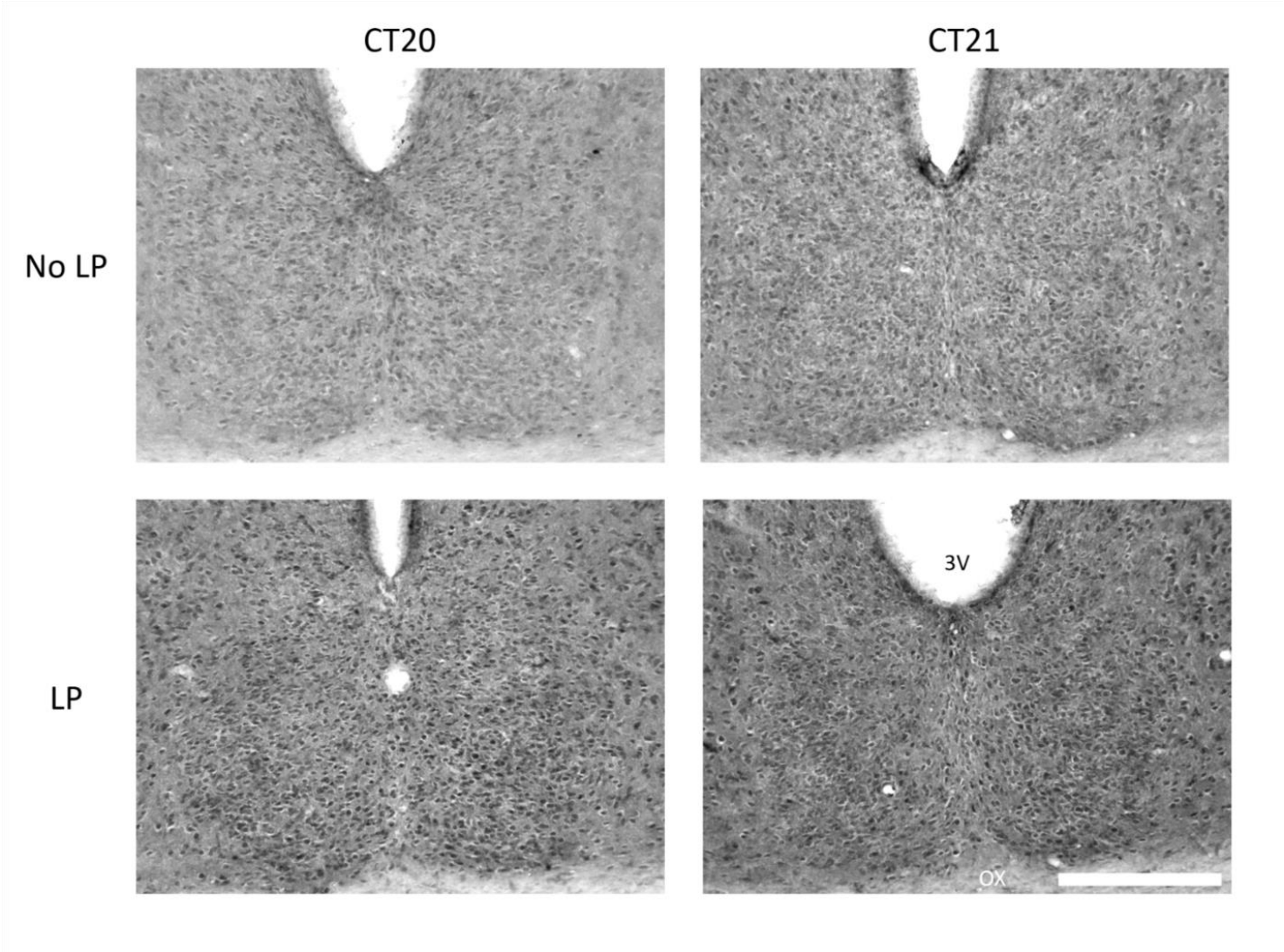

Figure 2.3. Representative coronal sections of the mid-caudal SCN exemplifying ATF4 protein expression. Hamsters were housed in constant darkness for 7 days prior to manipulation. Animals received either no LP or at LP at CT18 (15min at ~300lux) before being perfused at 2 hours (CT 20) or 3 hours (CT21) later. OX = optic chiasm, 3V = third ventricle, and the scale bar = 200μm.

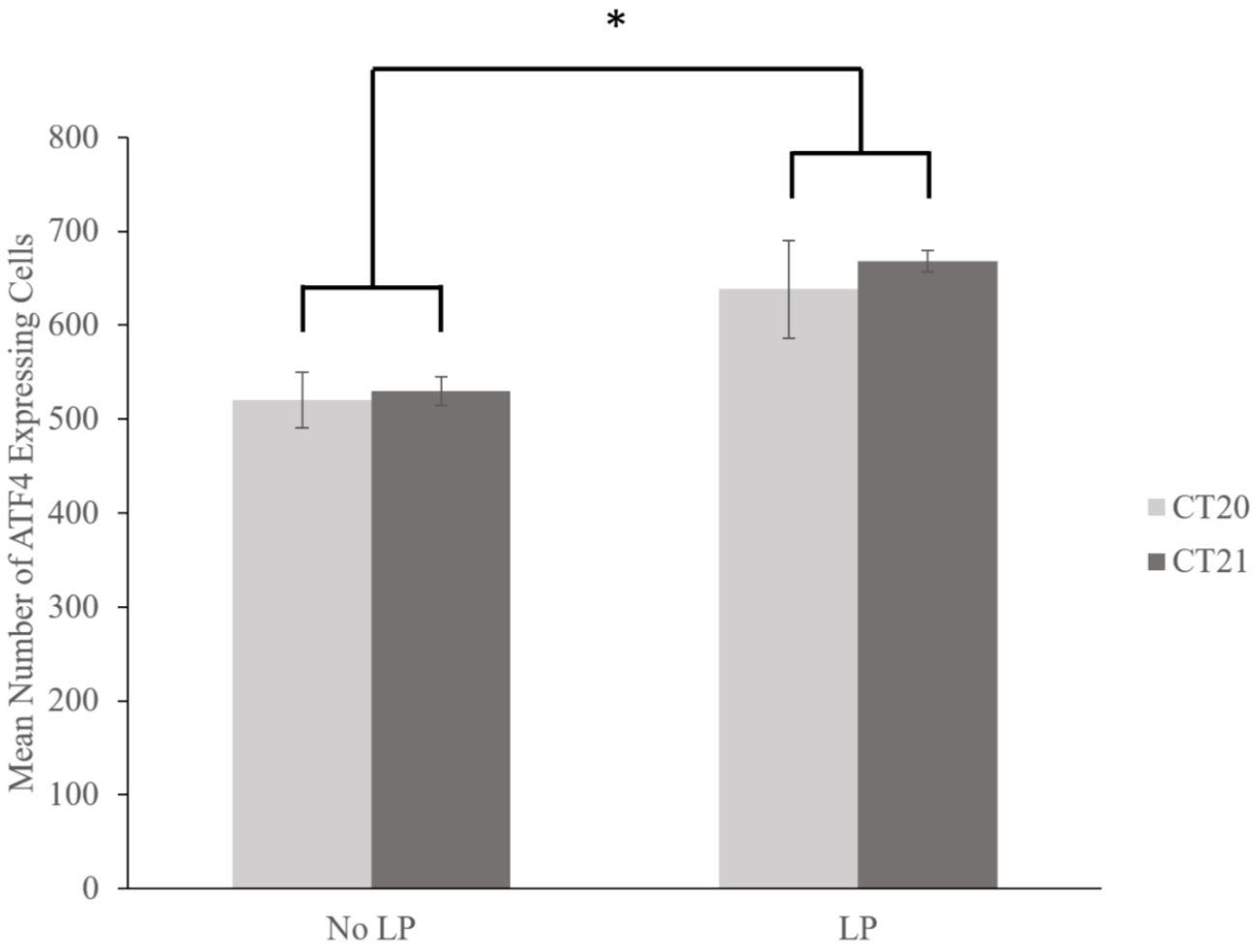

Figure 2.4. Mean manual cell count of the number of ATF4 protein expressing cells from hamsters receiving either no LP or a LP at CT18 (15min at ~300lux) before being perfused 2 hours (CT20) or 3 hours (CT21) later. Statistical significance of $p<.05$ was denoted by (*). Error bars represent ± SEM.

2.4 Discussion

The role of ATF4 in the mammalian circadian system has yet to be determined, therefore it was important to first examine the circadian profile of ATF4 in the SCN and the effect of light on its expression. It was found that ATF4 protein exhibited a circadian profile when hamsters were entrained to a 14:10 LD cycle (Figure 2.2A). Peak number of ATF4 cells were observed at ZT24, two hours following light phase onset (ZT22), and there were less ATF4 expressing cells at the subsequent time points until reaching the lowest levels at ZT18. This result was similar to previous mouse data showing *mAtf4* circadian expression peaked during the light phase (~ZT6) and were the lowest during the dark phase (~ZT18) (Koyanagi et al., 2011). The slight differences in the circadian profile may be due to species differences or using a LD cycle with a shorter dark phase; this may explain the earlier peak in ATF4 expression observed in hamsters. It must be noted that hamsters are recommended not to be housed in a 12:12 LD environment that is typical for mice as the increased dark phase would signal them to undergo preparations of hibernation resulting in potentially decreased locomotor activity (Hall et al., 1982).

When examining ATF4 protein expression of hamsters housed in constant darkness, there was no significant circadian rhythms observed (Figure 2.2B). This suggested that perhaps rhythmic ATF4 protein expression may be light driven. As hypothesized, results indicated that a CT18 light pulse significantly increased the number of ATF4 expressing cells observed by ~125% when compared to controls 2-3 hours following light exposure (Figure 2.4). Although purely speculative, this increased ATF4 expression at 2-3 hours following light exposure may be to limit the transcriptional activities of CREB on the CRE-elements of IEGs and clock genes, which begin almost immediately following light stimuli. However, further time points should be examined to test when this increased ATF4 expression returns to baseline. Overall, these results

indicate that the circadian expression of ATF4 protein in the SCN may be light driven suggesting that ATF4 may play a critical role in the photic phase resetting in the SCN.

Other interesting observations made, although they were not statistically quantified, were the observable localized spatial differences in ATF4 expressing cells with respect to the varying tested time points. When comparing ZT18 to ZT 24 slices, there were very few ATF4 expressing cells around the retinorecipient ventrolateral core region, whereas there appeared to be many more ATF4 expressing cells at ZT24 in the core (Figure 2.2A). Additionally, the signal in the core appeared to be much more pronounced and clustered at ZT24 when compared to ZT6 and ZT12 animals where it appeared more dispersed. ATF4 expression appeared to be persistent in the dorsomedial shell. The rhythmic expression in the core would further support the assertion that ATF4 expression may be light driven as the ventrolateral core neurons undergo various intracellular changes in response to photic signaling (Meijer and Schwartz, 2003; Antle et al., 2009). Additionally, ATF4 may be experiencing circadian expression in the shell as well, but DAB-IHC may not be a sensitive enough technique to detect this rhythm as signal is dependent on reaching a specific threshold of expression. This observation could be quantified by estimating the area of the two regions and quantifying the number of cells. A more reliable method would be the use of immunofluorescence using VIP and VP primary antibodies to label and differentiate core and shell neurons, respectively, that colocalize with ATF4 expressing cells.

Comparison among the three experiments must be done with caution because the CT expression and light-induced expression were completed using a second batch of primary ATF4-antibody that appeared to be less robust, thus requiring a higher concentration of 1:1000 and 1:250, respectively. When CT expression was compared to ZT expression tissue, ATF4 expression of hamsters in constant darkness appeared have more dispersed expression, a higher

number of observed cells, and weaker signal compared to animals in housed in LD (Figure 2.2B). This observation would warrant the interpretation that light may have an inhibitory effect on ATF4 expression in the core as there appeared to be more ATF4 expressing cells in absence of an LD cycle. However, this assertion would be contested with the significant increase in the number of ATF4 expressing cells due to brief light exposure when compared to controls (Figure 2.4). More likely, the secondary batch of primary ATF4 antibody produced a weaker signal requiring prolonged incubation in DAB, thus producing more noise and observable cells with a less robust signal. Interpretations comparing the three experiments lack reliability, therefore only interpretations of the experiments independently should be considered. In summary, ATF4 protein expression appeared to be rhythmic in LD, but not DD. There was increased ATF4 expression following brief light exposure. This data indicated that light may be crucial in driving ATF4 expression in the SCN of Syrian hamsters.

CHAPTER 3: ATF4 Downregulation in the SCN on Circadian Photic Phase Shifting

3.1 Introduction

The repressor activity of ATF4 on CREB makes it an attractive candidate when evaluating its effect on modulating photic phase shifts of the circadian clock. Research using the 5-HT mixed agonist/antagonists NAN-190 and BMY7378 has elucidated their ability to significantly potentiate photic phase advances, even when systemically administered after a light pulse (Byku and Gannon, 2000; Gannon, 2003; Lall and Harrington, 2006; Kessler et al., 2008). This suggested that these drugs may be exerting their effects downstream at the level of transcription and translation. Previous research investigating *c-fos*, *JunB*, and *Per1* expression downstream of the photic pathway indicated that 5-HT mixed agonist/antagonists may be prolonging their increased expression to light without further increasing levels of p-ERK and p-CREB beyond what is typical of a photic response (Recio et al., 1996; Smith et al. 2010, 2015b). CREB forms a positive feedback loop with itself by binding to its own CRE promoter, but also increases the expression of its repressor ATF4 (Hai and Hartman, 2001; Mohamed et al., 2005). ATF4 functions to repress p-CREB transcriptional activity by competitively binding to the CRE element of CREB resulting in the inhibition of CREB mRNA transcription (Hai and Hartman, 2001). It was hypothesized that photic-induction of CREB maybe prolonged through disinhibition by downregulation of ATF4 by using small interfering RNA (siRNA).

The following experiment utilized siRNA technology to downregulate ATF4 of the Syrian hamster (*Mesocricetus auratus*) under an Aschoff Type 2 design. The original reason for using the Syrian hamster was to replicate the potentiated phase advances previously observed when using 5-HT mixed agonist/antagonists. Additionally, surgical implantation of a cannula allowing for the repeated intracranial injections targeting the SCN are more easily performed in

hamsters compared to mice. Lastly, an Aschoff Type 2 design (manipulations in LD cycle) was used rather than an Aschoff Type 1 design (manipulations in constant darkness) because pilot data investigating the time-course of the use of siRNA (Appendix B) revealed that ATF4 may be changing the free running period (FRP) of the animal that may be masking the phase resetting effects of light. The Aschoff Type 2 design performs manipulations on animals in a LD cycle to maintain entrainment and control for changes in the FRP of the animal prior to being released into constant darkness and allowed to free run. Additionally, it allows us to investigate changes in locomotor activity and phase angle of entrainment in response to siRNA manipulations. It was hypothesized intracranial injections of ATF4 siRNA (siATF4) into the SCN would significantly potentiate phase shifts and/or alter phase angle of entrainment without affecting the level of locomotor activity. Analyzing these additional properties could provide better insight into the role of ATF4 in the mammalian master pacemaker.

3.2 Materials and Methods

3.2.1 Animals and Housing

This experiment used a total of 76 male Syrian Hamsters (*Mesocricetus auratus,* 110-180g). Fifty hamsters were utilized in the pilot studies that aimed to determine the correct dosage for the siRNA (n=24; Appendix A) and its time-course (n=26; Appendix B). Animals were supplied either from the Charles Rivers Labs (Kingston, NY) or through the ongoing breeding program in the lab. Animals arriving in the lab were given one week to acclimatize to the new environment, while the bred animals were required to reach the minimal weight prior to experimentation. Initially, animals were pair housed in polycarbonate cages (22x45x22 cm) at room temperature (21°C) in a 14:10 light-dark (LD) cycle with a cage level illuminance of

approximately 300 lux. Cages were changed bi-weekly, while food and water were provided ad libitum. Handling of animals in complete darkness during the experiment were done with the assistance of night vision goggles (BG15, Alista, Richmond Hill, Ontario, Canada). All protocols were approved by the University of Calgary Life and Environmental Sciences Animal Care committee and adhered to the Canadian Council Animal Care guidelines.

3.2.2 Intracranial Cannula Implantation Surgery

Stereotaxic cannula implantation surgeries were done on animals when the weight requirement was met (110g-180g). Animals were anesthetized with an intraperitoneal injection of sodium pentobarbital (120 mg/kg; CEVA) followed by a subcutaneous injection of butorphanol (2mg/kg; Wyeth) for pain management prior to surgery. Afterwards, animals were mounted on a Kopf stereotaxic frame (incisor bar set at -2.0mm below the interaural level) and provided oxygen (1L/min) supplemented with isoflurane (1-3%) with its body temperature (~35-37°C) maintained using a heated platform throughout the surgery. A 22-gauge stainless steel guide cannula (9mm long, Plastics One, Roanoke, VA) was implanted and targeted at the SCN (coordinates: +0.3mm anterior to bregma, +0.3mm lateral to midline, and -7.0mm ventral to the skull surface). A head cap was made to stabilize the cannula; three screws were drilled at a 45° angle to the plane of the skull in a triangular formation surrounding the cannula implant and stabilized by dental acrylic. A dust cap was inserted into the guide cannula to maintain patency. Both dust caps and injection cannulas extended 1mm beyond the end of the guide cannula. Animals were monitored and given at least one week of post-surgical recovery prior to experimentation.

3.2.3 Activity Rhythms

Following post-surgical recovery, hamsters were placed on a 14:10 LD cycle and given running wheels equipped with magnetic switches that are activated per wheel revolution. Graphical records of wheel running activity (actograms) were collected continuously using Clocklab Data Collection software (Coulbourn Instruments Allentown, PA). Activity onset was defined by the software as the first hour of activity bins that exceeded the 50th percentile of average activity after 5 hours of activity below the 50th percentile.

3.2.4 Small Interfering RNA (siRNA) and IntraSCN injections

Both the ATF4 silencer siRNA (siATF4) (10μg/1μL; Cat#: AM16706; Ambion) and the Missense siRNA (10μg/1μL; Cat#: AM4635; Ambion) were prepared by dissolving 40nmol siRNA in 26.6μL of RNase free water to obtain a 2x concentration (20μg/1μL) stock of each siRNA. These were separated into five 5μL aliquots and kept frozen at -20°C until required. Prior to manipulations, one aliquot would be thawed at 4°C for 30min followed by the addition of 5μL of DOTAP Liposomal Transfection Reagent (DOTAP; Ref#: 11202375001; Roche Diagnostics; Mannheim, Germany). The solution was gently mixed and allowed an incubation period of 30min at 4°C for siRNA incorporation into the transfection reagent. Using a 1μL Hamilton syringe attached to polyethylene 20 tubing with an injection cannula, intraSCN injections (0.5 μL) of either siATF4 or missense was administered over 30 seconds. The injector was held in the guide cannula for an additional 30 seconds to minimize the possibility of backflow. Workspace was cleaned with RNase Zap prior to injections and injection equipment were also wiped down with RNase Zap between injections to limit possibility of siRNA degradation.

3.2.5 Experimental Procedures

Hamsters were entrained to the 14:10 LD cycle and ensured to have stable activity onsets for at least 7 days prior to manipulation and release into constant darkness (Aschoff Type 2 design). The time-course pilot experiment (Appendix B) provided evidence that potentiated phase advances observed in siATF4 animals may have been due to a shortened FRP and the timing of the three-day injections were not controlled per animal, therefore the Aschoff Type 2 design aimed to maintain entrainment to the LD cycle following the siRNA injections and to control for the general timing of the siRNA injections.

Animals were separated into two groups; they were either given no LP or a LP at ZT18 (between-subjects factor). Animals in the no LP condition were released into constant darkness, while animals in the LP condition were subjected a phase advancing, full-room light pulse (~300lux for 15min) at ZT18 prior to being released into constant darkness. This was to determine the baseline responses of the animals to the two conditions. Animals were then allowed to free run until all animals had a stable FRP. Animals were then placed into a 14:10 LD cycle again and allowed to entrain. After seven days of stable entrainment, siRNA injections (missense or siATF4) were performed on animals in the both no LP and LP conditions over three days (one injection/day). Animals were given seven days following injections to recover in the LD cycle prior being given no LP or a LP at ZT18 again before being released into constant darkness and allowed to free run. Animals were allowed to free run until a stable FRP could be determined for all animals. Lastly, animals were placed back into a 14:10 LD cycle until stable entrainment was achieved. Again, animals were given the same siRNA injections depending on the treatment group they belonged to. This was followed by a seven day rest period in the LD cycle prior to a perfusion at ZT18 on the eighth day. Fixed brains were collected and subjected to

the DAB-IHC procedure to determine if siATF4 was successful in downregulating ATF4 expression in SCN neurons.

3.2.6 Analysis of Locomotor Activity, Phase Angle of Entrainment, and Phase Shifts

The daily locomotor activity, phase angle of entrainment, and phase shift data were collected on the Clocklab data collection software package (Coulbourn Instruments, Allentown, PA, USA) and analyzed using the Clocklab Analysis software. SigmaStat Version 2.03 (Systat Software, Inc.; San Jose, CA) was used to statistically evaluate the data with statistical significance set at $p<.05$. Post hoc comparisons were used to follow up all significant ANOVAs using the Student-Newman-Kuels test.

To determine if siRNA injections caused changes in locomotor activity, the average daily number of wheel revolutions five days prior to injections were averaged and compared to the average daily wheel running activity 5 days following the injections. Data from hamsters that appeared sick (head tilt) were not utilized because it could not be determined if changes in the frequency of wheel running activity was due to inability to run in the wheel caused by vestibular imbalances or the manipulation itself. Activity data pooled together regardless of light condition (n=19) was analyzed using a mixed 2 (Time: Pre-Injection, Post-Injection) x2 (Injection: Missense (n=9), siATF4 (n=10)) ANOVA to determine if there was a significant difference in the average locomotor activity between pre-injection and post-injection locomotor activity between the two siRNA conditions. Two planned comparisons were done to specifically compare the effect of siATF4 injection of changes in activity and the effect of missense injection of changes in activity.

Phase angle of entrainment was compared before and after siRNA injections (missense or siATF4). Phase angle was calculated by subtracting the activity onset from ZT12 (onset of dark

phase). Positive phase angle indicates that activity onset occurs prior to onset of the dark phase, while negative phase angle indicates activity onset occurs after. The phase angle of entrainment can provide evidence that the animals' endogenous FRP was affected by the siRNA injection, which would affect entrainment behaviour. The average phase angle of the five days before and five days after the manipulation were pooled together regardless of light condition (n=21) and were compared using a mixed 2 (Time: Pre-Injection, Post-Injection) x2 (Injection: Missense (n=10), siATF4 (n=11)) ANOVA. Two planned comparisons were done: 1) to specifically compare changes in phase angle within the siATF4 condition to compare pre-injection and post-injection phase angle, and 2) to compare phase angle of missense and siATF4 post-injection.

Lastly, behavioural phase shifts caused by experimental manipulations were analyzed by using Clocklab's automatic fitting function. Initially, animals were split into two groups, no LP or LP. Baseline responses to being released into DD or LP at ZT18 were analyzed. One regression line was fitted to activity onsets about 7 days prior to released into DD or LP, while the second regression line was fitted to activity onsets about 10 days following the manipulation. If a transience period was observed post manipulation, these unstable activity onsets were not used to fit the second regression line. The phase shift was calculated using the horizontal difference between the two regression lines on the day after being released into DD. Positive phase shifts represent phase advances, while negative phase shifts represent phase delays. These baseline measurements were particularly important to ensure animals simply began free running when released into DD, where as animals showed an expected phase advance to a baseline LP at ZT18. One animal did not show a phase advance to a LP and was reasoned to have had retinal damage due to prolonged surgical time; it was removed from the study. To analyze how siRNA injections affected these two baseline responses, one regression line was fitted to activity onsets

about 7 days prior to siRNA injections, while the second regression line was fitted using stable activity onsets 10 days of data following being simply released in to DD (no LP; n=10) or released into DD after a light pulse at ZT18 (n=10). Again, the phase shift was calculated using the horizontal difference between the two regression lines on the day after being released into DD. A mixed 2 (Light condition: no LP, LP) x3 (Injection: no injection/Missense/siATF4) ANOVA was used to determine if siATF4 would significantly change the response of animals to a LP. Three planned comparisons were done to compare the effect of light on missense and siATF4 injections, and comparisons between no injection, missense, and siATF4 injections within the no light condition.

3.2.7 Immunohistochemistry

After the experiment, diaminobenzidine (DAB)- immunohistochemistry (IHC) protocol was used to determine cannula placement and analyze if siATF4 was effective in downregulating ATF4 expression in the SCN. Hamsters were deeply anesthetized using 0.4mL of sodium pentobarbital (Euthanyl, MTC Pharmaceuticals, Cambridge, ON, Canada). Hamsters were first perfused intracardially with ~100mL of cold phosphate buffered saline (PBS) followed by ~100mL of 4% paraformaldehyde to fix the tissue. Brains were removed and placed in 4% paraformaldehyde solution for another ~18-24hrs to allow for further fixation. Brains were then cryoprotected in a 20% sucrose solution at 4°C for a minimum of 48 hours.

The DAB-IHC protocol used was based on previous studies from our laboratory (Antle et al., 2008). All rinses were done on a shaker tray unless otherwise specified. Alternating brain sections were sliced and collected at 35μm using a Leica Cyrostat at -18°C and were placed in plastic/nylon wells filled with phosphate buffered saline (PBS). To inactivate endogenous peroxidases, sections were rinsed for 15 min in 0.5% H_2O_2 in PBSx (PBS with 0.3% Triton X-

100) and then rinsed three times with PBSx for 10min each. Afterwards, slices were incubated in 5% normal goat serum in PBSx followed by a 48hr incubation at 4°C in the primary antibody for ATF4 (rabbit anti-ATF4 (human); 1:4000; PA5-19521; Invitrogen). Tissue slices were then subjected to three 10min rinses with PBSx, 1hr incubation in the secondary antibody biotinylated goat anti-rabbit (1:200; Vector Laboratories, Burlingame, CA, USA), three more 10 min PBSx rinses, a 1hr incubation in ABC (Vectastain Elite kit, Vector Laboratories, Burlingame, CA, USA), and another 10min PBSx rinses. For approximately 15-45min, slices were developed in 24mL of 0.1M Tris buffer, 0.05% DAB, and 0.02% NiCl solution that was activated by 80μL of 30% H_2O_2. Slices were mounted on to gelatin-coated slides, air-dried for at least 1hr, dehydrated through an alcohol series, cleared with xylenes, and cover slipped with Permount.

3.2.8 Cannula Placement and Quantification of ATF4 Expression

Images of the DAB stained brain tissue were captured using a 20x objective on an Olympus BX51 microscope equipped with a QICam Fast 1394 digital video camera (QImaging, Burnaby, BC, Canada). Hamsters were included in the data analysis only if the cannula tip was within 500µm of the SCN. ATF4 expression was analyzed by the manual cell counting function on ImageJ 1.34s (National Institutes of Health, Bethesda, MD, USA). One representative slice of the central caudal SCN, determined by anatomical shape and tissue integrity, from each animal was selected for analysis of cellular ATF4 protein expression. The coronal slices of central-caudal SCN were selected because it contained both the dorsomedial shell and the ventrolateral core neuronal populations of the SCN (Card and Moore, 1984). To standardize counting area, an elliptical shape (width=200µm, height=250µm) was used as the boundary for the manual cell counting. The number ATF4 expressing cells were compared between animals receiving a missense or siATF4 injection using an independent t-test to analyze if siATF4 effectively

downregulated ATF4 expression in the SCN. Although cannula placement was determined for all hamsters, only hamsters from the LP condition (n=10) were used in the analysis because it used the first batch of primary ATF4 antibody that was more robust.

3.3 Results

3.3.1 Analysis of Circadian Properties

The mean daily locomotor activity, measured in total wheel running activity per day, before and after siRNA injections were compared using a mixed 2 (Time: Pre-Injection, Post-Injection) x2 (Injection: Missense, siATF4) ANOVA mixed ANOVA (Figure 3.1). It was hypothesized that only siATF4 injections would significantly decrease mean locomotor activity following injections, however this was not supported as the interaction between time and siRNA injection was not a significant ($F_{1,17}$=3.840, p=.067; Figure 3.2). Rather, there was a significant main effect of injection ($F_{1,17}$=24.374, p<.001), in which the injection, regardless of type, caused a significant decrease in mean locomotor activity when comparing pre-injection (M=5447.69, SEM=732.21) to post-injection (M=2217.16, SEM=298.03). Animals in the missense group (M=3395.11, SEM=657.64) did not significantly differ in overall locomotor activity when compared to the siATF4 group (M=4269.74, SEM=623.89) because time did not have a significant main effect ($F_{1,17}$=.931, p=.348). With the planned comparisons, it was found that missense injections did not significantly decrease in activity when comparing pre-injection to post-injection conditions (p=.056). However, within the siATF4 condition there was significant decrease in activity when comparing pre-injection to post-injection conditions (p<.001).

The phase angle of entrainment before and after siRNA injections were compared using a mixed 2 (Time: Pre-Injection, Post-Injection) x2 (Injection: Missense, siATF4) ANOVA (Figure 3.1). Based on the time-course pilot study (Appendix B), it was hypothesized that siATF4 would cause a significant change in phase angle when compared to the missense treatment group. This hypothesis was supported by a significant interaction between injection time and injection ($F_{1,19}$=4.814, p=.041; Figure 3.3). This significant interaction was further analyzed using Student-Newman-Kuels post hoc comparisons. Within the siATF4 condition, the phase angle of entrainment was significantly more positive post-injection (M=1.11, SEM=.56) relative to pre-injection (M=-.07, SEM=.05; p=.007). There was no significant difference in phase angle when comparing pre-injection (M=.07, SEM=.13) with post-injection (M=.02, SEM=.13) within the missense condition (p=.796). There was no significant difference in pre-injection phase angle when comparing missense to siATF4 (p=.444), but siATF4 produced a significantly more positive phase angle than missense post-injection (p=.018).

The effect of siATF4 on potentiating photic phase shifts was assessed by a mixed 2 (Light condition: no LP, LP) x3 (Injection: no injection/Missense/siATF4) ANOVA (Figure 3.4). Although it was hypothesized that only siATF4 would significantly potentiate photic phase advances, there was no significant interaction between light condition and siRNA injection ($F_{2,15}$=.211, p=.812; Figure 3.5). As predicted, light (M=2.10, SEM=.17) significantly potentiated phase shifts compared to the no light condition when averaged over the injection condition (M=.44, SEM=.17; $F_{1,15}$=48.185, p<.001). Additionally, there was a significant main effect of injection condition ($F_{2,15}$=5.240, p=.019). Averaged over light condition, siATF4 injections (M=2.01, SEM=.27) produced significantly larger phase shifts than both no injection (M=1.01, SEM=.16; p=.006) and missense injection (M=.80, SEM=.29; p=.020) conditions. More

specifically within the LP condition, siATF4 injection (*M*=2.84, *SEM*=.43) did not significantly potentiate phase advances when compared to missense injection (*M*=1.52, *SEM*=.37; *p*=.084). However, within the no LP condition, siATF4 injections (*M*=1.18, *SEM*=.34) alone significantly produced larger phase shifts than the no injection (*M*=.09, *SEM*=.22; *p*=.016), but not when compared with the missense injection (*M*=.07, *SEM*=.44; *p*=.143) condition.

Figure 3.1. Representative actograms of running wheel activity of hamsters injected at ZT18 with either missense (A) or siATF4 (B, C) to show changes in magnitude of locomotor activity and phase angle of entrainment pre-injection compared to post-injection. Each horizontal line represents a different day, while the vertical black marks portray the magnitude of wheel running activity. Areas of white represent the light phase, while areas of grey represent the dark phase. The orange line represents the average activity onsets calculated 5 days pre-injection, while the blue line represents the average activity onset calculated 5 days post-injection. The difference between the average activity onsets and the onset of the dark phase is the phase angle of entrainment. The green box ( ) represents the three consecutive days of missense injections, while the purple box ( ) represents the three consecutive days of siATF4 injections.

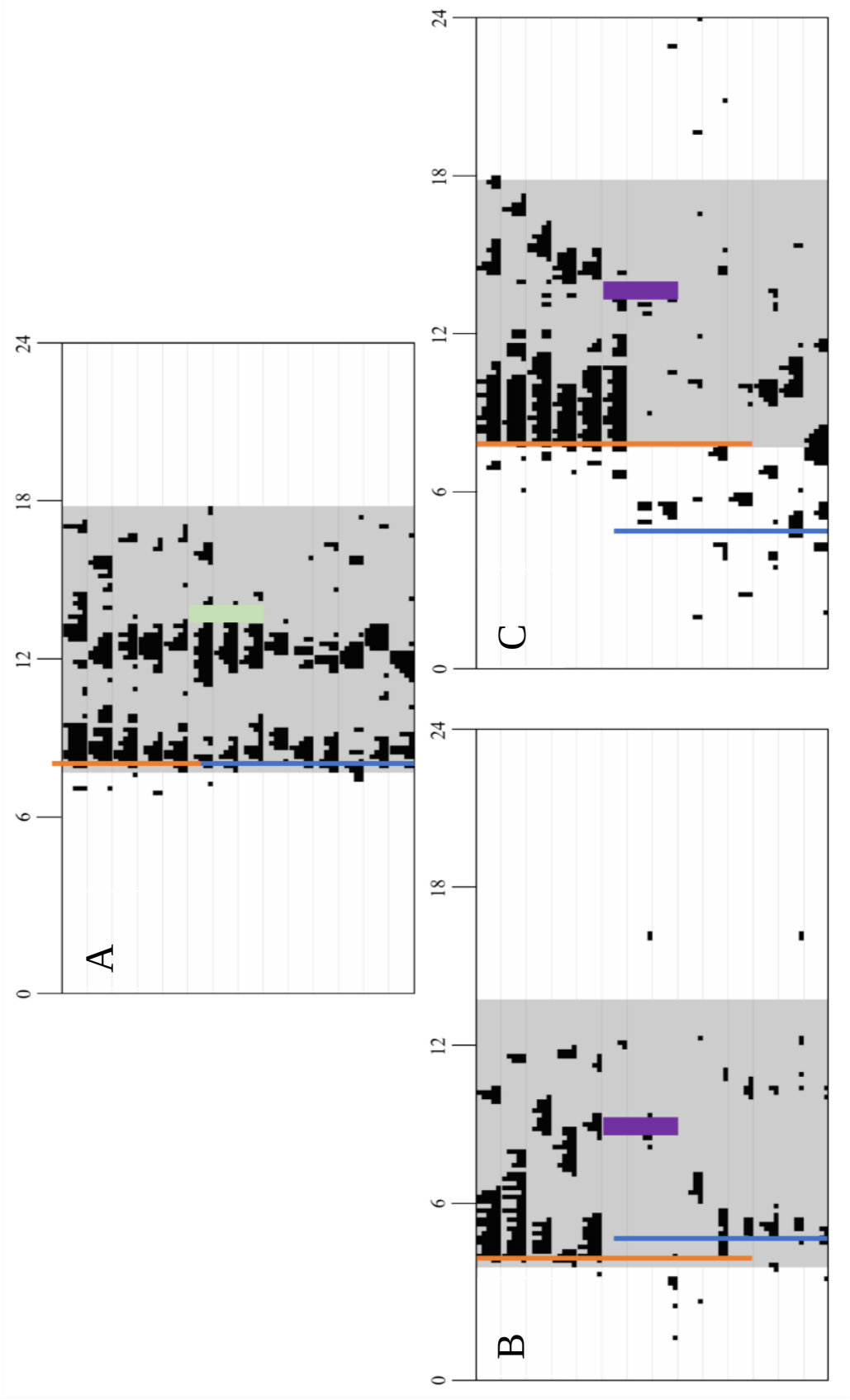
A
B
C
0
6
12
18
24

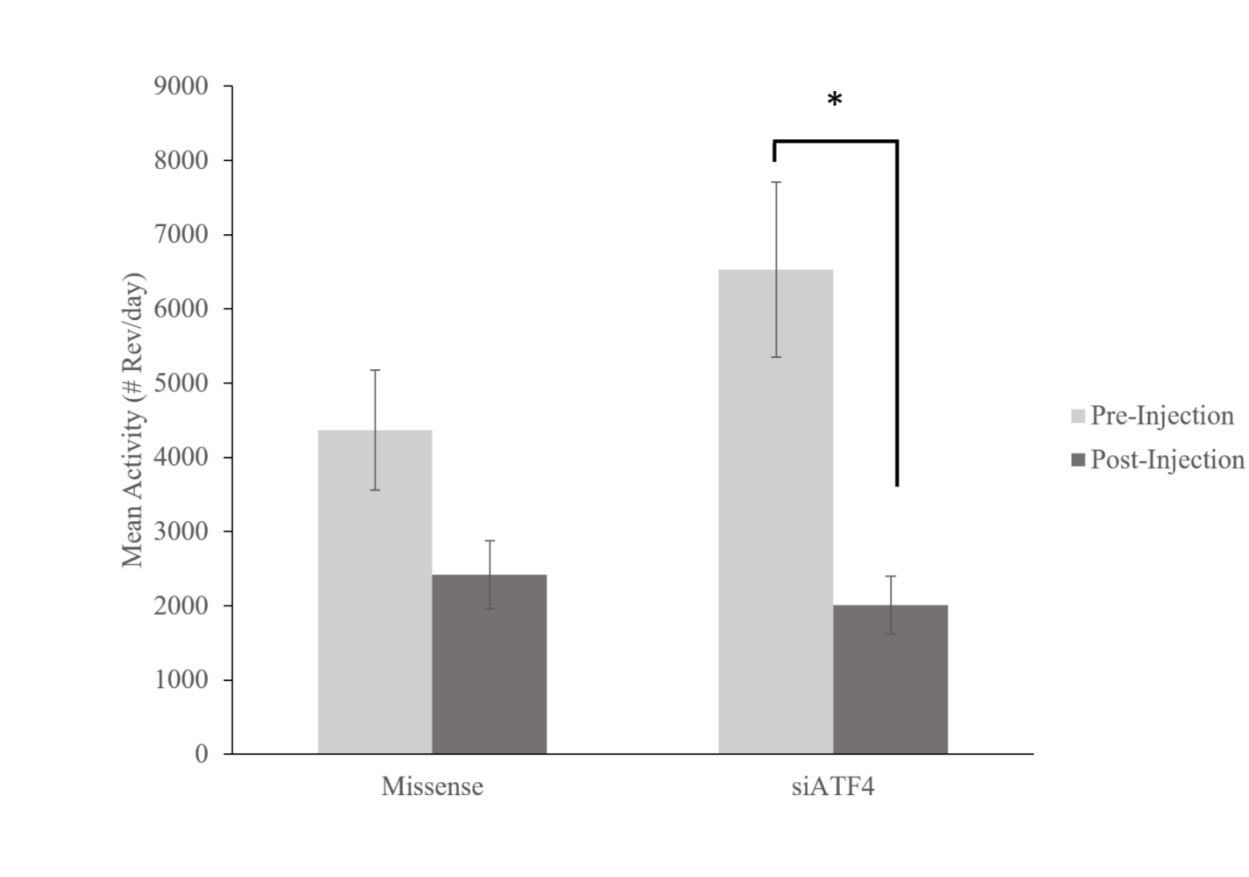

Figure 3.2. Mean level of pre-injection and post-injection locomotor activity of hamsters receiving either missense or siATF4 injections. Locomotor activity was measured in the number of wheel revolutions per day. Statistical significance of $p<.05$ was denoted by (*). Error bars represent ± SEM.

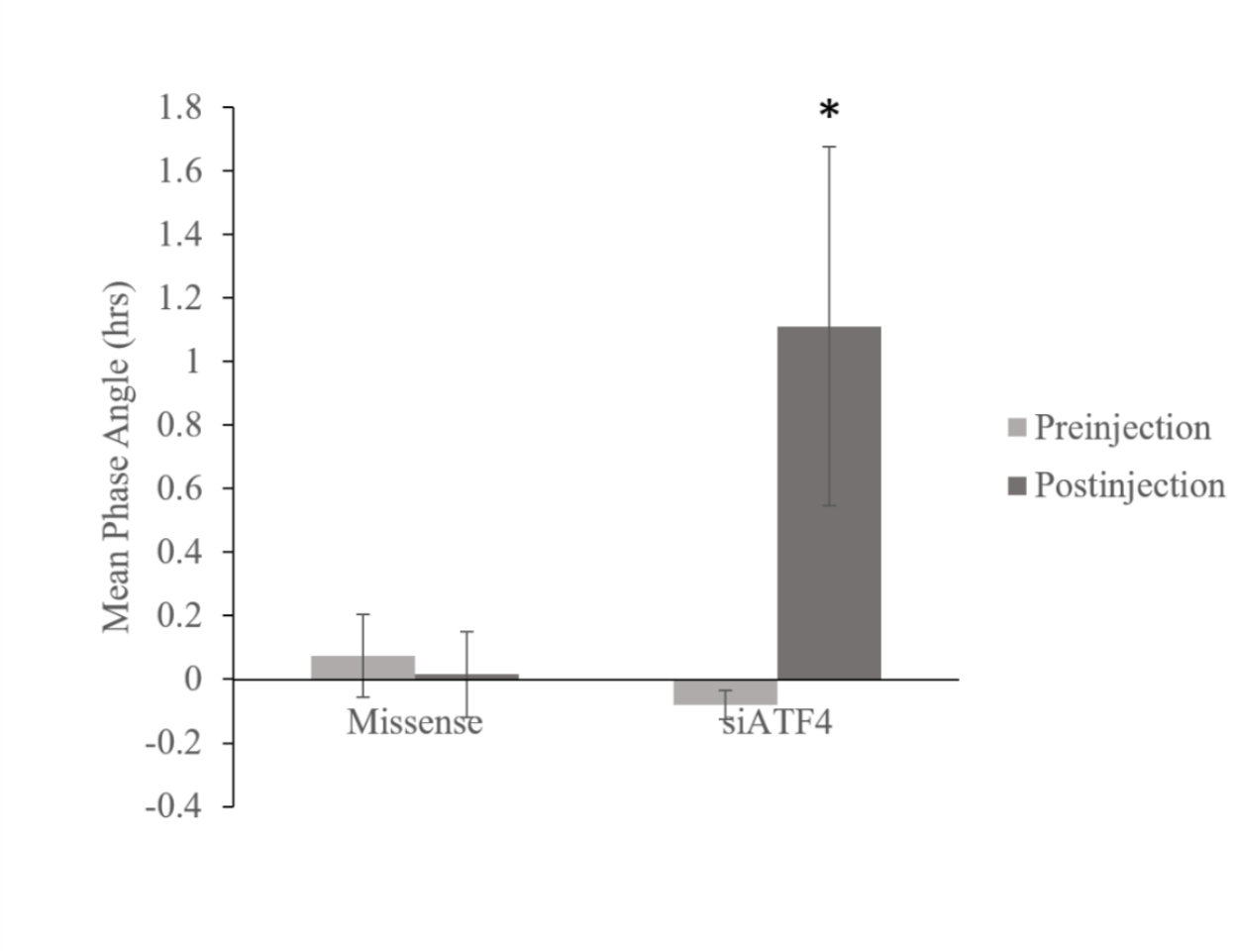

Figure 3.3. Mean phase angle of entrainment pre-injection and post-injection of hamsters receiving either missense or siATF4 injections. Phase angle was calculated by the difference from the average 5 days of activity onsets by the onset of the dark phase. Statistical significance of $p<.05$ was denoted by (*). Error bars represent ± SEM.

Figure 3.4. Representative actograms of running wheel activity of three hamsters when given no injection (A,C,E) or injected at ZT18 with either missense (B) or siATF4 (D,F) prior to being released in to constant darkness (no LP) 7 days after siRNA manipulation. Actograms vertically aligned were from the same animal (ie. A and B, C and D, E and F). Each horizontal line represents a different day, while the vertical black marks portray the magnitude of wheel running activity. Areas of white represent the light phase, while areas of grey represent the dark phase. The orange line represents the regression line fitted to activity onsets 5 days pre-injection and the blue line represents the regression line fitted to stable activity onsets after being released into constant darkness. Phase shifts were calculated by using the difference between the two trend lines on the first day following being released into constant darkness. The green box ( ) represents the three consecutive days of missense injections, while the purple box ( ) represents the three consecutive days of siATF4 injections.

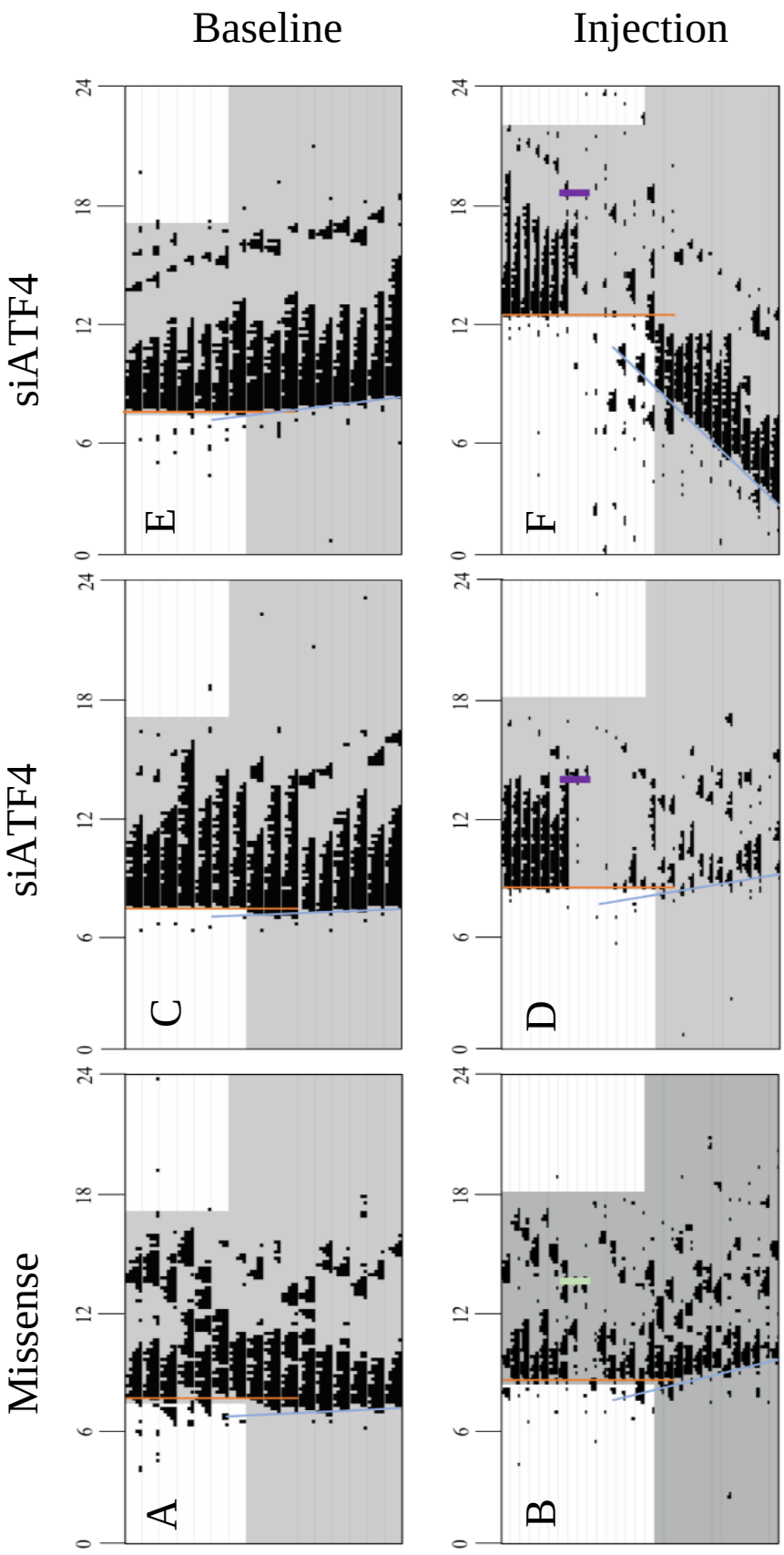
Baseline
Injection
siATF4
siATF4
Missense
A
B
C
D
E
F
0
6
12
18
24

Figure 3.5. Representative actograms of running wheel activity of three hamsters, when given no injection (A,C) or injected at ZT18 with either missense (B) or siATF4 (D), prior to being given a phase advancing light pulse at ZT18 (LP) 7 days following siRNA manipulation and then being released in to constant darkness. Actograms vertically aligned were from the same animal (ie. A and B, C and D). Each horizontal line represents a different day, while the vertical black marks portray the magnitude of wheel running activity. Areas of white represent the light phase, while areas of grey represent the dark phase. The orange line represents the regression line fitted to activity onsets 5 days pre-injection and the blue line represents the regression line fitted to stable activity onsets after being released into constant darkness. Phase shifts were calculated by using the difference between the two trend lines on the first day following being released into constant darkness. The green box (□) represents the three consecutive days of missense injections, the white box (□) represents the light pulse (15 min at ~300lux), and the purple box (□) represents the three consecutive days of siATF4 injections.

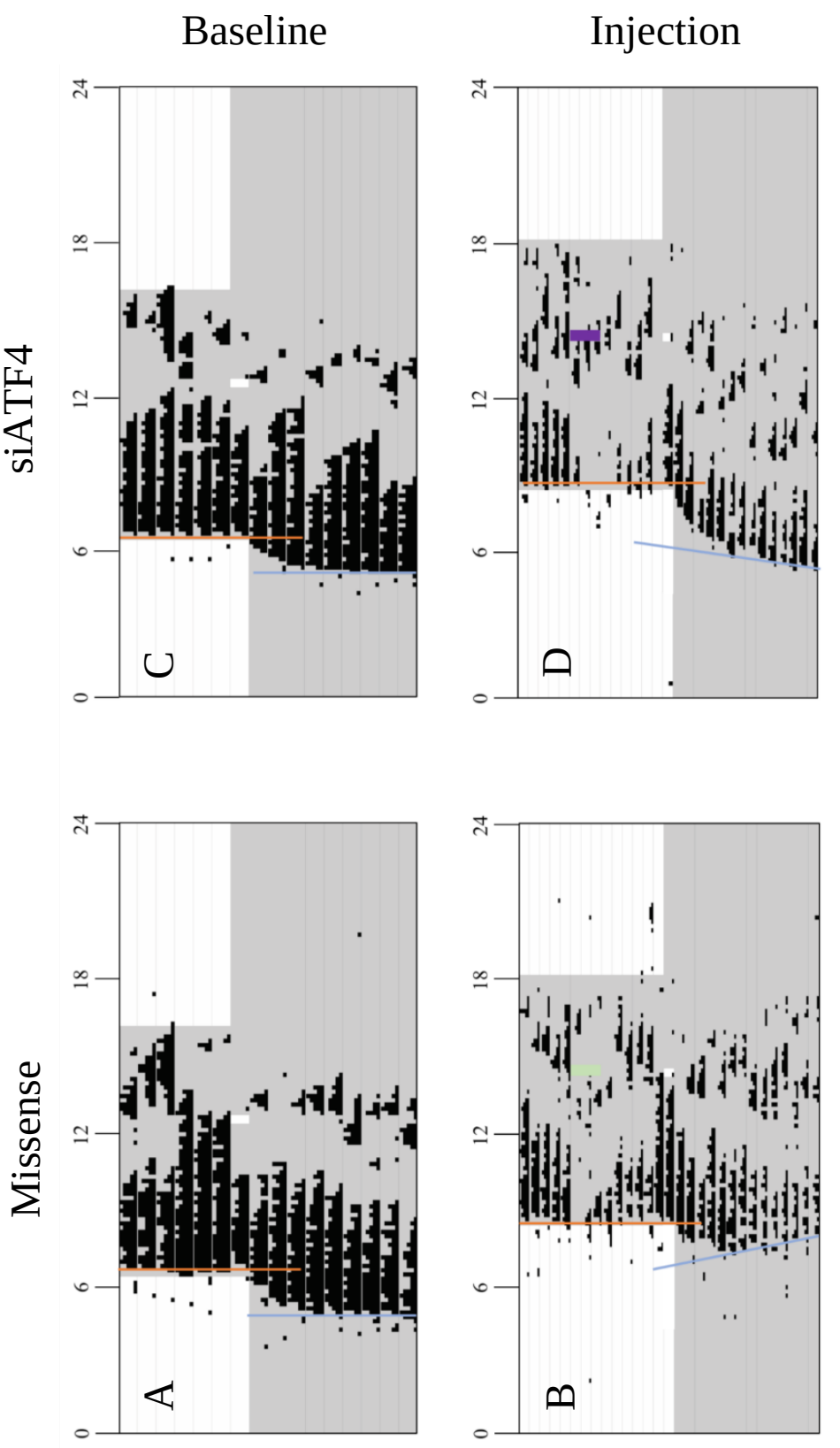
Baseline
Injection
siATF4
Missense
A
B
C
D
0
6
12
18
24

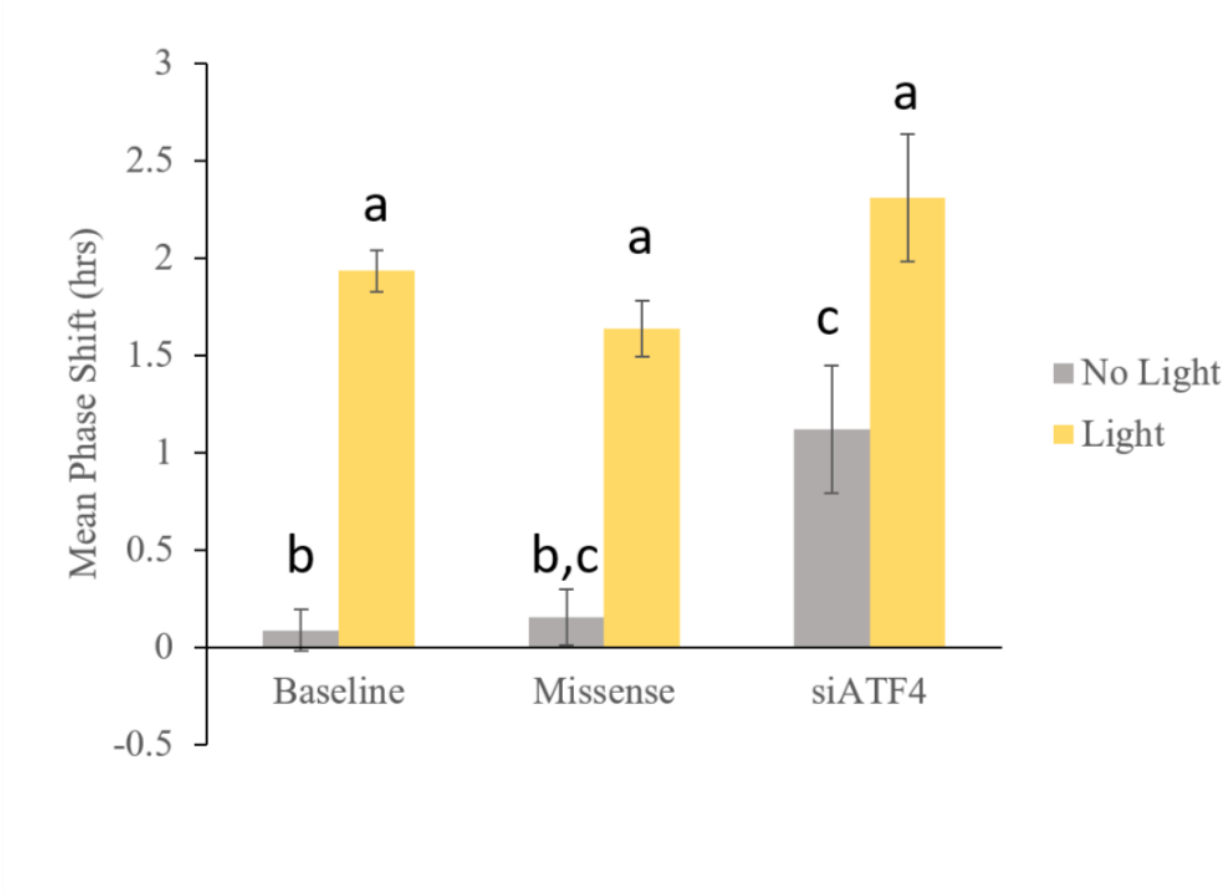

Figure 3.6. Mean phase shifts of hamsters receiving no injection, missense, or siATF4 injections prior to being released in constant darkness (no LP) seven days later or given a phase advancing light pulse at ZT18 (LP; 15 min at ~300lux). Bars not sharing a letter are significantly different from each other ($p<.05$). Error bars represent ± SEM.

3.3.2 Efficacy of siRNA in Downregulating ATF4 expression in the SCN

To determine if siATF4 was overall effective in downregulating ATF4 expression in the SCN, an independent t-test was used to analyze the number of ATF4 expressing cells in the SCN after DAB-IHC (Figure 3.6). It was hypothesized that siATF4 would significantly reduce the number of ATF4 expressing cells in the SCN. However, results indicated that siATF4 (*M*=426.50, *SEM*=32.92) did not significantly reduce the number of ATF4 expressing cells in the SCN when compared to missense injections (*M*=494.80, *SEM*=33.56; t_9=1.442, *p*=.183; Figure 3.7).

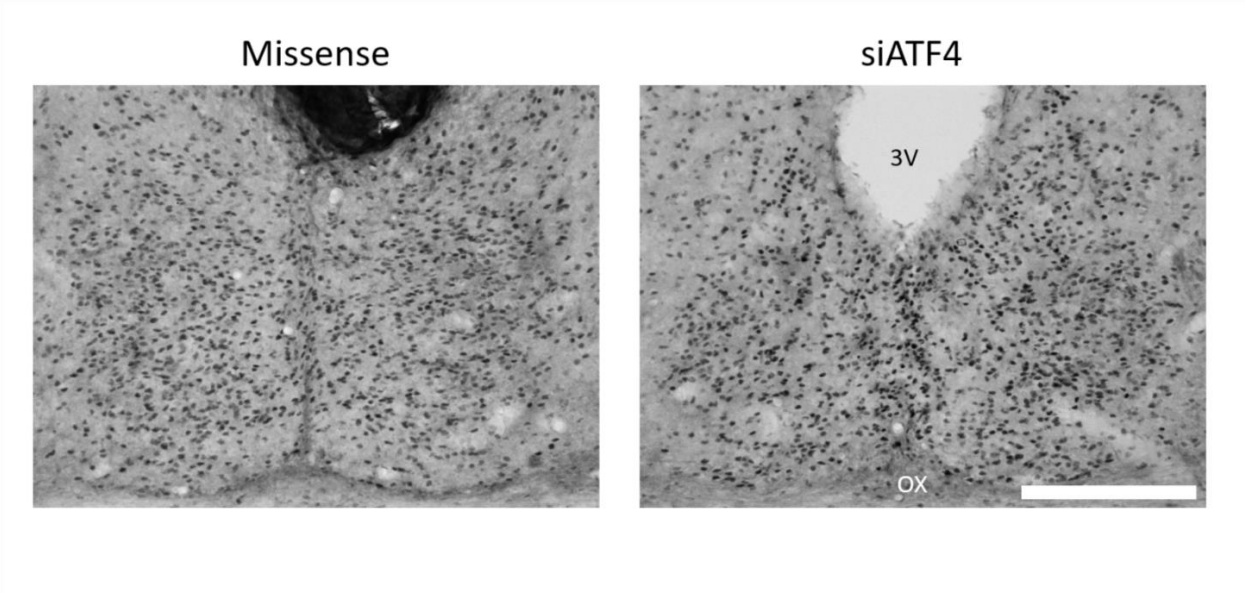

Figure 3.7. Representative coronal sections of the mid-caudal SCN exemplifying ATF4 protein expression of hamsters 7 days after receiving intracranial injections of either missense or siATF4. OX = optic chiasm, 3V = third ventricle, and the scale bar = 200µm.

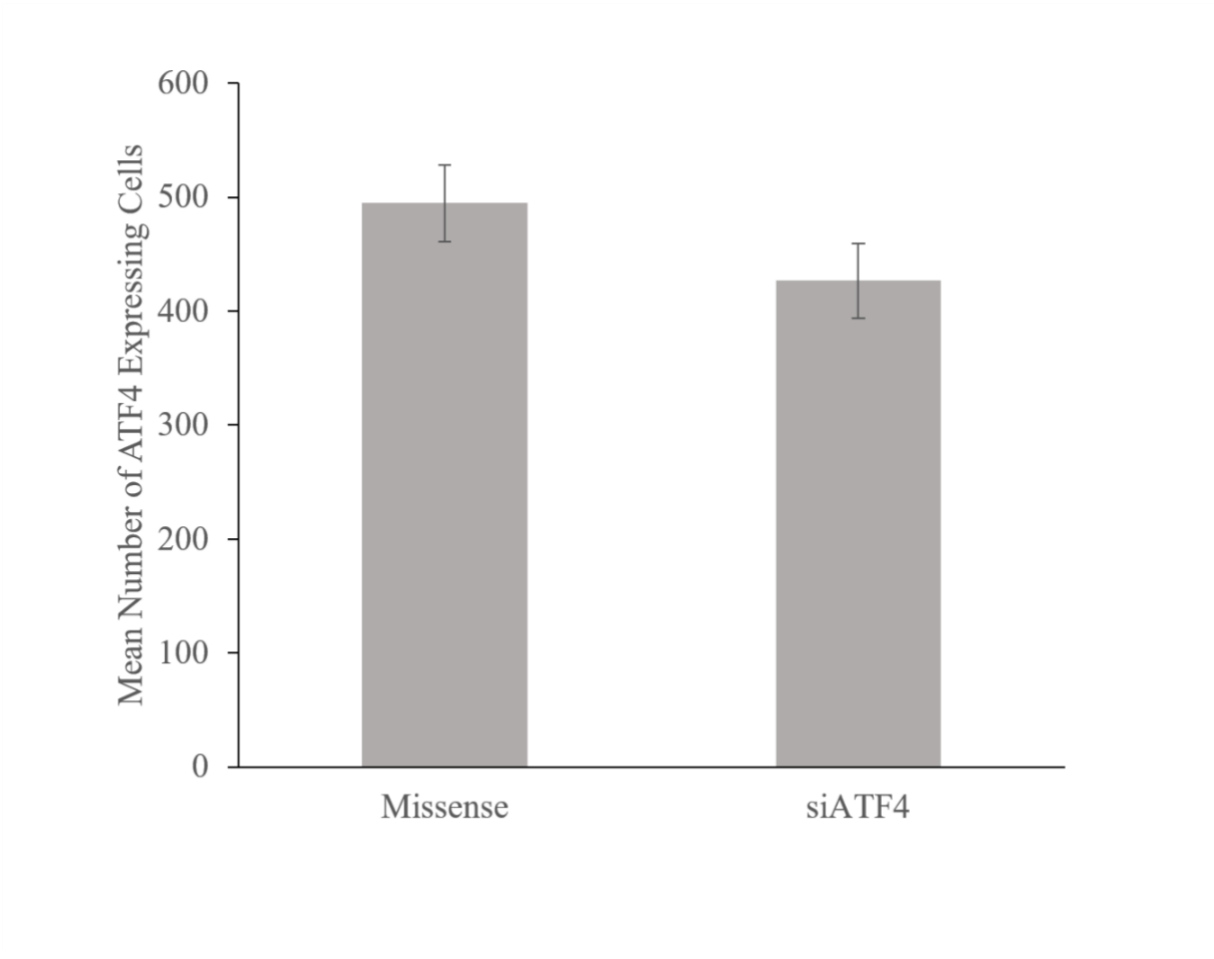

Figure 3.8. Mean manual cell count of the number of ATF4 protein expressing cells from hamsters 7 days after receiving intracranial injections of either missense or siATF4. Error bars represent ± SEM.

3.4 Discussion

Previous research using siRNA technology to induce changes in circadian behavioural in hamsters had not yet been done, therefore it was necessary to design a protocol that may be sufficient in elucidating an effect. From two pilot studies (Appendix A and B), a siRNA concentration ($10\mu g/1\mu L$) and time-course (ie. significantly large phase advances were observed when a LP was given at CT18 seven days after siRNA manipulation) were estimated. It was observed from the time-course pilot experiment that hamsters may be experiencing changes in their free running period (FRP) prior to light exposure, which may be attributed to the potentiated photic phase advances observed (Appendix B). This was difficult to distinguish when animals could free run under the Aschoff type 1 design.

With the current Aschoff type 2 design, it was hypothesized that hamsters housed in an LD cycle would maintain entrainment following siRNA manipulation and exhibit potentiated phase advances to light exposure. However, results indicated that a light pulse did not significantly potentiate phase advances in siATF4 animals when compared to baseline and missense injections (Figure 3.6). Surprisingly, siATF4 injections alone showed the ability to cause phase advances. When examining the phase angle of entrainment, siATF4 animals exhibited significantly large positive angle of entrainment when compared to the pre-injection condition and missense condition (Figure 3.3). Additionally, it was the act of injections that produced a significant decrease in locomotor activity regardless of which siRNA injection received (Figure 3.2). Animals with phase shifts to siATF4 alone were likely artifacts of this positive phase angle as the free running rhythm would have a more positive start point. Having a large positive phase angle prior to being released into constant darkness looks like a phase shift since the pre-injection activity onsets were used rather than the post-injection activity onsets. As

a result, interpreting phase shifts due to siATF4 injections alone lacks validity as it is likely due to the increase in phase angle of entrainment. However, phase angle of entrainment can be used to determine the endogenous FRP of an animal (Dunlap et al., 2004). A positive phase angle is indicative of a shorter FRP, therefore downregulation of ATF4 in the SCN may be significantly shortening the FRP of these animals. This interpretation is consistent with research suggesting that ATF4 is more important in rhythmic expression as a target of CLOCK and a direct regulator of *Per2* transcription (Igarashi et al., 2007; Koyanagi et al., 2011). Decreased ATF4 levels would result in less PER2 production attributing to a shorter period in the TTFL and a "faster" clock. Since other clock genes should hypothetically be functional, this observation further supports the theory that ATF4 is a more dominant regulator of *Per2* than CLOCK-BMAL1. Therefore, ATF4 activity may play a critical role in determining circadian period rather than the photic resetting of the clock.

The main caveat in this experiment was that siATF4 did not significantly decrease the number of ATF4 expressing cells when compared to missense (Figure 3.8). Since there was a significant effect of siATF4 on phase angle, there were three factors that needed to be considered. First, DAB-IHC and manual cell counting may not be sensitive enough to observe the downregulation of ATF4 that may be occurring within the individual cells as signal can be produced as long as ATF4 expression meets a certain threshold. Unfortunately, DAB-IHC was required because it allowed for the spatial resolution to determine correct cannula placements. Still, utilizing western blots may allow for more sensitive quantification of ATF4 protein expression through the analysis of relative optical density comparing missense to siATF4 conditions. Second, only animals that received a LP were used to evaluate the efficacy of downregulating ATF4 using siATF4. This was because analysis of LP group utilized the first

batch of primary ATF4-antibody, whereas the no LP group was done at a later time using the second batch of primary ATF4-antibody in which the signal was not as robust. Less subjects would result in less statistical power. Lastly, the criteria requiring cannula placement to be within 500μm of the SCN may not be stringent enough to elicit sufficient downregulation of ATF4. This can be exemplified by the noteworthy variability observed in phase angle of entrainment (Figure 3.1; B vs C) and phase shifts with no light pulse (Figure 3.4; D vs F) of siATF4 treated animals. Furthermore, it was observed that the most extreme changes in phase angle were from animals that had the entire SCN completely infused with the siATF4, but this resulted in unusable SCN tissue to use for cell counting. Research has been shown that the network properties of the SCN help maintain circadian stability and robustness even in the presence of genetic mutations and tissue damage (Mohawk and Takahashi, 2011). In SCN chimeras made from wild-type and circadian mutant (ie. Tau mutant tissue have shorter periods, while Clock Δ19 mutants have longer periods) tissue, it was found that behavioural rhythmicity persisted, but often in an intermediate period of the two cell types (Vogelbaum' and Menaker, 1992; Nakamura et al., 2002). Additionally, circadian rhythmicity can persist even if 20% of the nuclei remains intact after SCN ablation (Rusak, 1977). Also, cannula implantations were only unilaterally implanted, therefore intraSCN injections of ATF4 may not be affecting enough SCN neurons, especially those in the ventrolateral core and contralateral to the infusion site, to induce a significant circadian effect since SCN cells have been shown to be so robust to changes in rhythmicity.

Since ATF4 is a repressor of CREB, then it should be very likely that photic resetting should be affected in some way, therefore there maybe other reasons that may be explored to explain the lack of effect siATF4 had on photic phase resetting. One factor that might be

considered is that ATF4 maybe more influential on the phase delay portion of the PRC as ATF4 has been found to preferentially target the CRE promotor of the *Per2* gene, which has been found to exhibit significant increase following light pulse during the early subjective night (Hirota and Fukada, 2004). Another point to mention would be that if downregulating ATF4 affects the overall period of the clock, it maybe changing the phase response curve (PRC) by shortening it. For animals that experienced significant downregulation of ATF4, it may be possible that light exposure at ZT18 may not be occurring at the peak phase advancing region of the PRC leading to a smaller phase advance. These two considerations could be explored simply by giving LP during the early subjective night (ZT13) and earlier times in the late subjective night (ZT15-17) 7 days after siATF4 injections.

Although it was not specifically examined, it is very unlikely that serotonin mixed agonist/antagonists exert its potentiating effect on phase advances by affecting ATF4. This is highlighted by the fact that the FRP of the animals were not significantly affected in previous experiments, whereas our results suggest that ATF4 plays a more significant role in affecting FRP (Lall and Harrington, 2006; Kessler et al., 2008; Lungwitz and Gannon, 2009). Additionally, siATF4 injections did not potentiate phase advances as previously seen, although there were many caveats that needed to be taken into consideration as stated above. However, the siRNAs are said to downregulate their targets longer (ie. ~2-3 weeks in neuronal tissue because it is dependent on cellular turnover rate) than drugs targeting peptide receptors; this may explain these behavioural differences because prolonged downregulation of ATF4 would inhibit the ability to return to the previous FRP and potentially mask photic phase shifts. Using shRNAs with shorter downregulation latencies may potentially be used to address this problem. However, it would be important to examine if serotonin mixed agonist/antagonists exert their potentiating

effects by altering ATF4 expression in the SCN. A time-course experiment to evaluate changes in protein expression after systemic injections of BMY7378 or NAN-190 followed by light exposure testing should be done, similar to Smith et al. (2015b). This could give us more insight to determine if ATF4 plays a role in photic resetting of the clock.

In summary, downregulation of ATF4 using siATF4 was found not to potentiate photic phase advances, but it significant changed the phase angle of entrainment. This effect was not attributed to the significant decrease in locomotor activity as lower locomotor activity was observed in both missense and siATF4 injections. Protocol modifications specifically dealing with the spatial accuracy of implantation and temporal accuracy of light exposure should be explored due to the huge variability of the results. Lastly, based on the behavioural circadian effects observed in this study, it is very unlikely that serotonergic mixed agonist/antagonists are affecting ATF4 to exert its potentiating effect on photic phase advances.

CHAPTER 4: GENERAL DISCUSSION

4.1 Overall Conclusions

This investigation provided new insight into the role of ATF4 in the mammalian circadian system. The results suggest that ATF4 protein expression in Syrian hamsters exhibits circadian rhythmicity with peak levels occurring during the early light phase (~ZT24) and its lowest levels occurring during the late subjective night (~ZT18). This mirrors previous research into the circadian expression profile of *mAtf4* (Koyanagi et al., 2011). Circadian expression of ATF4 was not observed in constant darkness suggesting that light may be driving the circadian rhythmicity of ATF4 expression. This was further supported by data suggesting that a light pulse presented at CT18 was sufficient to increase the number of ATF4 SCN cells observed 2-3 hours following light exposure. This was consistent with the hypothesis that ATF4 plays an inhibitory role to light-induced CREB expression as increased ATF4 expression may be occurring to limit light-induced CREB transcriptional activity on IEGs and clock genes.

In exploring the effects of ATF4 downregulation using siRNA technology, the administration of siATF4 into the SCN did not significantly potentiate photic phase advances. If ATF4 acted as a repressor to light-induced CREB activity, one would expect that downregulation of ATF4 would allow for prolonged CREB activity and potentiate photic phase shifts. However, a lack of observed potentiated phase shifts indicated that ATF4 may not actually be behaving as a "brake" to light-induced CREB transcriptional activity as previously hypothesized. The function of the light-induced increase of ATF4 expression observed in experiment 3 is still unknown. Rather, siATF4 injections significantly affected phase angle of entrainment, and as consequence, the free running period (FRP). This observation was consistent with previous

research indicating that ATF4 was a direct target of CLOCK and also directly regulated PER2 expression, both core components of the TTFL (Igarashi et al., 2007; Koyanagi et al., 2011). Collectively, this investigation provided some evidence to support the contention that ATF4 is playing an important role in maintaining the rhythmicity of the clock. However, these results were weakened by the lack of observable downregulation of ATF4 expressing cells by siATF4 in the DAB-IHC analysis. The observed changes in phase angle cannot be attributed to the downregulation of ATF4, but can only be attributed to the siATF4 injection itself. Therefore, interpretations made from these observations must be exercised with caution and further investigation is warranted.

4.2 Limitations and Future Directions

When it was observed that rhythmic expression of ATF4 may be light-driven in the ventrolateral SCN core from experiment 1, it revealed the possible heterogeneity of ATF4 expression and function. Although the current studies suggest that ATF4 may not be important in the light-induced pathway to the SCN, it may be a result of procedural limitations. First, the use of DAB-IHC to evaluate ATF4 protein expression through cell counting may not have been sensitive enough to visualize ATF4 downregulation in the SCN. This technique does not directly quantify protein levels; if siATF4 downregulates ATF4 levels in the SCN, but not below the threshold, a signal can still be observed. Therefore, it could not be statistically determined that the significant effects of siATF4 injections on phase angle were specifically due to ATF4 downregulation. Second, there are no antibodies nor siRNAs produced specifically for the Syrian hamster, which may hinder its robustness in terms of antibody signal and effectiveness of protein downregulation. Third, cannula placement using the 500μm criteria may have been too liberal for effective siRNA transfection to occur in the majority of SCN cells, and perhaps leading to the

large variability observed in the results. Lastly, siRNA infusion using a catatonic liposomal agent (ie. DOTAP) as the method of delivery would hypothetically affect the SCN cells globally, therefore the function of ATF4 with regards to the heterogeneity of SCN cell types could not be addressed. When approaching the problem with cellular and genetic specificity, it would be important to consider the mouse model as there are significantly more genetic tools available.

The mouse model and its genetic tools were originally not considered due to the limited data regarding the role of ATF4 in the SCN; it did not warrant heavy investment into genetically modified mice. To provide more evidence into its role, surgical cannula implantation with siRNA injections was the more economic technique because it allows for repeated manipulations in a repeated measures design. However, this surgery is more difficult perform in mice and the original hypothesis for the project came from the serotonergic agonist/antagonist experiments which used Syrian hamsters (Byku and Gannon, 2000; Kessler et al., 2008; Lungwitz and Gannon, 2009; Smith et al., 2010, 2015b). When these serotonergic drugs were injected into mice, the potentiation of photic phase shifts was not as robust as those observed in hamsters (Smith et al., 2010). Thus, the Syrian hamster was chosen as the model organism.

For future investigation, the primary objective would be to develop a more specific technique targeting ATF4 expression of core and shell neurons separately, and to use a more sensitive assay to confirm ATF4 downregulation. Downregulation of ATF4 expression in specific cells of the SCN could potentially be achieved using Cre recombinase and siRNA technology (Kasim, 2004). There are VIP-Cre and AVP-Cre transgenic mice with immunofluorescent reporter constructs available that could specifically express Cre recombinase in the retinorecipient VIP core neurons and the rhythmic AVP shell neurons, respectively. Viral infusions (ie. Adeno-associated virus or Lentivirus) using Cre ON-siATF4-GFP vector

constructs requiring Cre recombinase for activation could be infused into the SCN (Kasim, 2004). In the VIP-Cre mice, only the VIP cells of the SCN would be able to cleave and activate the siATF4 from the vector to be incorporated into the RISC complex, the endogenous mRNA cleaving machinery. This would hopefully lead to the downregulation of ATF4 specifically in VIP neurons of the core. Similarly, this could be done with AVP-Cre mice to target downregulation of ATF4 in the shell. Successful transfection of the vector could be determined through the colocalization of the florescent reporters with immunofluorescence. If successful, this could be used to evaluate the function of ATF4 in different SCN neuronal populations and the effect of siATF4 downregulation on behavioural circadian outputs of the clock.

4.3 Clinical Importance

Circadian desynchronization is extremely prevalent in society often caused by shift work, frequent intercontinental travel resulting in jetlag, and circadian disorders. Circadian desynchronization results in numerous health consequences including increased risk of cardiovascular disease, breast cancer, metabolic diseases, mental disorders, and decreased attention and vigilance leading to increased risk of workplace accidents (Mistlberger et al., 2000; Knutsson, 2003; Dunlap et al., 2004). Chronobiotics aim to increase photic resetting efficiency and normalize circadian abnormalities to mitigate the negative consequences of circadian desynchronization. The current investigation highlights the importance of ATF4 in controlling rhythmicity. Further research into the circadian role of ATF4 and associated pathways could implicate ATF4 as a novel target for developing chronobiotics. Various FDA-approved serotonergic drugs have shown some promise in modulating the clock, but the intracellular mechanisms remain unknown. This type of research would economically increase the pharmacological tools available to address the health problems of circadian desynchronization.

REFERENCES

Abe M, Herzog ED, Yamazaki S, Straume M, Tei H, Sakaki Y, Menaker M (2002) Circadian Rhythms in Isolated Brain Regions. Journal of Neuroscience 22:350–356.

Albrecht U, Sun ZS, Eichele G, Lee CC (1997) A differential response of two putative mammalian circadian regulators, mper1and mper2, to light. Cell 91:1055–1064.

Ameri K, Harris AL (2008) Activating transcription factor 4. The International Journal of Biochemistry & Cell Biology 40:14–21.

Antle MC, Ogilvie MD, Pickard GE, Mistlberger RE (2003) Response of the mouse circadian system to serotonin 1A/2/7 agonists in vivo: surprisingly little. J Biol Rhythms 18:145–158.

Antle MC, Silver R (2005) Orchestrating time: arrangements of the brain circadian clock. Trends in Neurosciences 28:145–151.

Antle MC, Smith VM, Sterniczuk R, Yamakawa GR, Rakai BD (2009) Physiological responses of the circadian clock to acute light exposure at night. Reviews in Endocrine and Metabolic Disorders 10:279–291.

Antle MC, Tse F, Koke SJ, Sterniczuk R, Hagel K (2008) Non-photic phase shifting of the circadian clock: role of the extracellular signal-responsive kinases I/II/mitogen-activated protein kinase pathway. Eur J Neurosci 28:2511–2518.

Aschoff J (1951) [Determination of loco-motor activity of mice by mechanical rectifier]. Pflugers Arch Gesamte Physiol Menschen Tiere 254:262–266.

Bartsch D, Casadio A, Karl KA, Serodio P, Kandel ER (1998) CREB1 encodes a nuclear activator, a repressor, and a cytoplasmic modulator that form a regulatory unit critical for long-term facilitation. Cell 95:211–223.

Bartsch D, Ghirardi M, Skehel PA, Karl KA, Herder SP, Chen M, Bailey CH, Kandel ER (1995) Aplysia CREB2 represses long-term facilitation: relief of repression converts transient facilitation into long-term functional and structural change. Cell 83:979–992.

Brown TM, Piggins HD (2007) Electrophysiology of the suprachiasmatic circadian clock. Progress in Neurobiology 82:229–255.

Bryant DN, LeSauter J, Silver R, Romero M-T (2000) Retinal Innervation of Calbindin-D28K Cells in the Hamster Suprachiasmatic Nucleus: Ultrastructural Characterization. Journal of Biological Rhythms 15:103–111.

Butcher GQ, Dziema H, Collamore M, Burgoon PW, Obrietan K (2002) The p42/44 Mitogen-activated Protein Kinase Pathway Couples Photic Input to Circadian Clock Entrainment. Journal of Biological Chemistry 277:29519–29525.

Byku M, Gannon RL (2000) Effects of the 5HT1A agonist/antagonist BMY 7378 on light-induced phase advances in hamster circadian activity rhythms during aging. J Biol Rhythms 15:300–305.

Card JP, Brecha N, Karten HJ, Moore RY (1981) Immunocytochemical localization of vasoactive intestinal polypeptide-containing cells and processes in the suprachiasmatic nucleus of the rat: light and electron microscopic analysis. J Neurosci 1:1289–1303.

Card JP, Moore RY (1984) The suprachiasmatic nucleus of the golden hamster: Immunohistochemical analysis of cell and fiber distribution. Neuroscience 13:415–431.

Chan RK, Sterniczuk R, Enkhbold Y, Jeffers RT, Basu P, Duong B, Chow SL, Smith VM, Antle MC (2016) Phase shifts to light are altered by antagonists to neuropeptide receptors. Neuroscience 327:115–124.

Chen A, Muzzio IA, Malleret G, Bartsch D, Verbitsky M, Pavlidis P, Yonan AL, Vronskaya S, Grody MB, Cepeda I (2003) Inducible enhancement of memory storage and synaptic plasticity in transgenic mice expressing an inhibitor of ATF4 (CREB-2) and C/EBP proteins. Neuron 39:655–669.

Chevray PM, Nathans D (1992) Protein interaction cloning in yeast: identification of mammalian proteins that react with the leucine zipper of Jun. Proc Natl Acad Sci USA 89:5789–5793.

Daikoku S, Hisano S, Kagotani Y (1992) Neuronal associations in the rat suprachiasmatic nucleus demonstrated by immunoelectron microscopy. The Journal of Comparative Neurology 325:559–571.

Dardente H, Poirel VJ, Klosen P, Pévet P, Masson-Pévet M (2002) Per and neuropeptide expression in the rat suprachiasmatic nuclei: compartmentalization and differential cellular induction by light. Brain Research 958:261–271.

DeCoursey PJ, Buggy J (1989) Circadian rhythmicity after neural transplant to hamster third ventricle: specificity of suprachiasmatic nuclei. Brain Research 500:263–275.

Deutsch PJ, Hoeffler JP, Jameson JL, Lin JC, Habener JF (1988) Structural determinants for transcriptional activation by cAMP-responsive DNA elements. J Biol Chem 263:18466–18472.

Ding JM, Chen D, Weber ET, Faiman LE, Rea MA, Gillette MU (1994) Resetting the biological clock: mediation of nocturnal circadian shifts by glutamate and NO. Science-AAAS-Weekly Paper Edition 266:1713–1716.

Drucker-Colín R, Aguilar-Roblero R, García-Hernández F, Fernández-Cancino F, Rattoni FB (1984) Fetal suprachiasmatic nucleus transplants: diurnal rhythm recovery of lesioned rats. Brain Research 311:353–357.

Dudley TE, DiNardo LA, Glass JD (1998) Endogenous regulation of serotonin release in the hamster suprachiasmatic nucleus. J Neurosci 18:5045–5052.

Dunlap JC, Loros, J. J. , & DeCoursey, P.J., ed (2004) Chronobiology: Biological Timekeeping. Sunderland, Massachusetts, USA: Sinauer Associates, Inc. Publishers.

Dziema H, Obrietan K (2002) PACAP potentiates L-type calcium channel conductance in suprachiasmatic nucleus neurons by activating the MAPK pathway. Journal of neurophysiology 88:1374–1386.

Eastman CI, Tomaka VA, Crowley SJ (2017) Sex and ancestry determine the free-running circadian period. Journal of Sleep Research 26:547–550.

Edery I (2000) Circadian rhythms in a nutshell. Physiological Genomics 3:59–74.

Fukunaga K, Horikawa K, Shibata S, Takeuchi Y, Miyamoto E (2002) Ca2+/calmodulin-dependent protein kinase II-dependent long-term potentiation in the rat suprachiasmatic nucleus and its inhibition by melatonin. J Neurosci Res 70:799–807.

Gallego M, Virshup DM (2007) Post-translational modifications regulate the ticking of the circadian clock. Nature Reviews Molecular Cell Biology 8:139–148.

Gannon R. (2003) Serotonergic serotonin1A mixed agonists/antagonists elicit large-magnitude phase shifts in hamster circadian wheel-running rhythms. Neuroscience 119:567–576.

Gannon RL, Millan MJ (2006) Serotonin1A autoreceptor activation by S 15535 enhances circadian activity rhythms in hamsters: Evaluation of potential interactions with serotonin2A and serotonin2C receptors. Neuroscience 137:287–299.

Gau D, Lemberger T, von Gall C, Kretz O, Le Minh N, Gass P, Schmid W, Schibler U, Korf HW, Schütz G (2002) Phosphorylation of CREB Ser142 Regulates Light-Induced Phase Shifts of the Circadian Clock. Neuron 34:245–253.

Gekakis N, Staknis D, Nguyen HB, Davis FC, Wilsbacher LD, King DP, Takahashi JS, Weitz CJ (1998) Role of the CLOCK protein in the mammalian circadian mechanism. Science 280:1564–1569.

Ginty DD, Kornhauser JM, Thompson MA, Bading H, Mayo KE, Takahashi JS, Greenbergf ME (1993) Regulation of CREB Phosphorylation in the Suprachiasmatic Nucleus by Light. Science 260:9.

Gooley JJ, Lu J, Chou TC, Scammell TE, Saper CB (2001) Melanopsin in cells of origin of the retinohypothalamic tract. Nat Neurosci 4:1165.

Guido ME, Goguen D, De Guido L, Robertson HA, Rusak B (1999) Circadian and photic regulation of immediate-early gene expression in the hamster suprachiasmatic nucleus. Neuroscience 90:555–571.

Güldner FH (1976) Synaptology of the rat suprachiasmatic nucleus. Cell Tissue Res 165:509–544.

Güler AD, Ecker JL, Lall GS, Haq S, Altimus CM, Liao HW, Barnard AR, Cahill H, Badea TC, Zhao H, Hankins MW, Berson DM, Lucas RJ, Yau KW, Hattar S (2008) Melanopsin cells are the principal conduits for rod–cone input to non-image-forming vision. Nature 453:102–105.

Hai T, Curran T (1991) Cross-family dimerization of transcription factors Fos/Jun and ATF/CREB alters DNA binding specificity. Proc Natl Acad Sci USA 88:3720–3724.

Hai T, Hartman MG (2001) The molecular biology and nomenclature of the activating transcription factor/cAMP responsive element binding family of transcription factors: activating transcription factor proteins and homeostasis. Gene 273:1–11.

Hall VD, Bartke A, Goldman BD (1982) Role of the testis in regulating the duration of hibernation in the Turkish hamster, Mesocricetus brandti. Biol Reprod 27:802–810.

Hamada T, Antle MC, Silver R (2004) Temporal and spatial expression patterns of canonical clock genes and clock-controlled genes in the suprachiasmatic nucleus. European Journal of Neuroscience 19:1741–1748.

Hamada T, LeSauter J, Venuti JM, Silver R (2001) Expression of Period genes: rhythmic and nonrhythmic compartments of the suprachiasmatic nucleus pacemaker. Journal of Neuroscience 21:7742–7750.

Hannibal J (2006) Roles of PACAP-Containing Retinal Ganglion Cells in Circadian Timing. In: International Review of Cytology, pp 1–39. Elsevier.

Harrington ME (1997) The ventral lateral geniculate nucleus and the intergeniculate leaflet: interrelated structures in the visual and circadian systems. Neurosci Biobehav Rev 21:705–727.

Harrington ME, Rahmani T, Lee CA (1993) Effects of damage to SCN neurons and efferent pathways on circadian activity rhythms of hamsters. Brain Res Bull 30:655–669.

Herzog ED, Takahashi JS, Block GD (1998) Clock controls circadian period in isolated suprachiasmatic nucleus neurons. Nature Neuroscience 1:708–713.

Hirota T, Fukada Y (2004) Resetting Mechanism of Central and Peripheral Circadian Clocks in Mammals. Zoological Science 21:359–368.

Honma S, Shirakawa T, Katsuno Y, Namihira M, Honma K (1998) Circadian periods of single suprachiasmatic neurons in rats. Neuroscience Letters 250:157–160.

Ibata Y, Okamura H, Tanaka M, Tamada Y, Hayashi S, Iijima N, Matsuda T, Munekawa K, Takamatsu T, Hisa Y, Shigeyoshi Y, Amaya F (1999) Functional Morphology of the Suprachiasmatic Nucleus. Frontiers in Neuroendocrinology 20:241–268.

Ibata Y, Tanaka M, Ichitani Y, Takahashi Y, Okamura H (1993) Neuronal interaction between VIP and vasopressin neurones in the rat suprachiasmatic nucleus. Neuroreport 4:128–130.

Igarashi T, Izumi H, Uchiumi T, Nishio K, Arao T, Tanabe M, Uramoto H, Sugio K, Yasumoto K, Sasaguri Y, others (2007) Clock and ATF4 transcription system regulates drug resistance in human cancer cell lines. Oncogene 26:4749–4760.

Inouye ST, Kawamura H (1979) Persistence of circadian rhythmicity in a mammalian hypothalamic “island” containing the suprachiasmatic nucleus. Proceedings of the National Academy of Sciences 76:5962–5966.

Jiang ZG, Teshima K, Yang Y, Yoshioka T, Allen CN (2000) Pre- and postsynaptic actions of serotonin on rat suprachiasmatic nucleus neurons. Brain Res 866:247–256.

Johnson MS (1926) Activity and distribution of certain wild mice in relation to biotic communities. J Mammal. 7: 254-277.

Johnson MS (1939) Effect of continuous light on periodic spontaneous activity of white-footed mice (*Permyscus*). J Exp Zool. 82: 315-328.

Karpinski BA, Morle GD, Huggenvik J, Uhler MD, Leiden JM (1992) Molecular cloning of human CREB-2: an ATF/CREB transcription factor that can negatively regulate

transcription from the cAMP response element. Proceedings of the National Academy of Sciences 89:4820–4824.

Kasim V (2004) Control of siRNA expression using the Cre-loxP recombination system. Nucleic Acids Research 32:e66–e66.

Kennaway DJ, Rowe SA, Ferguson SA (1996) Serotonin agonists mimic the phase shifting effects of light on the melatonin rhythm in rats. Brain Res 737:301–307.

Kessler EJ, Sprouse J, Harrington ME (2008) NAN-190 potentiates the circadian response to light and speeds re-entrainment to advanced light cycles. Neuroscience 154:1187–1194.

King DP, Zhao Y, Sangoram AM, Wilsbacher LD, Tanaka M, Antoch MP, Steeves TD, Vitaterna MH, Kornhauser JM, Lowrey PL (1997) Positional cloning of the mouse circadian clock gene. Cell 89:641–653.

Knutsson A (2003) Health disorders of shift workers. Occupational Medicine 53:103–108.

Kornhauser JM, Nelson DE, Mayo KE, Takahashi JS (1990) Photic and circadian regulation of c-fos gene expression in the hamster suprachiasmatic nucleus. Neuron 5:127–134.

Koyanagi S, Hamdan AM, Horiguchi M, Kusunose N, Okamoto A, Matsunaga N, Ohdo S (2011) cAMP-response Element (CRE)-mediated Transcription by Activating Transcription Factor-4 (ATF4) Is Essential for Circadian Expression of the Period2 Gene. Journal of Biological Chemistry 286:32416–32423.

Kume K, Zylka MJ, Sriram S, Shearman LP, Weaver DR, Jin X, Maywood ES, Hastings MH, Reppert SM (1999) mCRY1 and mCRY2 are essential components of the negative limb of the circadian clock feedback loop. Cell 98:193–205.

Lall GS, Harrington ME (2006) Potentiation of the resetting effects of light on circadian rhythms of hamsters using serotonin and neuropeptide Y receptor antagonists. Neuroscience 141:1545–1552.

Lassot I, Estrabaud E, Emiliani S, Benkirane M, Benarous R, Margottin-Goguet F (2005) p300 modulates ATF4 stability and transcriptional activity independently of its acetyltransferase domain. J Biol Chem 280:41537–41545.

Lassot I, Ségéral E, Berlioz-Torrent C, Durand H, Groussin L, Hai T, Benarous R, Margottin-Goguet F (2001) ATF4 degradation relies on a phosphorylation-dependent interaction with the SCF(betaTrCP) ubiquitin ligase. Mol Cell Biol 21:2192–2202.

Leak RK, Card JP, Moore RY (1999) Suprachiasmatic pacemaker organization analyzed by viral transynaptic transport. Brain Research 819:23–32.

Lee C, Etchegaray JP, Cagampang FR, Loudon AS, Reppert SM (2001) Posttranslational mechanisms regulate the mammalian circadian clock. Cell 107:855–867.

Lee HS, Nelms JL, Nguyen M, Silver R, Lehman MN (2003) The eye is necessary for a circadian rhythm in the suprachiasmatic nucleus. Nature Neuroscience 6:111–112.

LeSauter J, Kriegsfeld L., Hon J, Silver R (2002) Calbindin-D28K cells selectively contact intra-SCN neurons. Neuroscience 111:575–585.

Lin YS, Green MR (1988) Interaction of a common cellular transcription factor, ATF, with regulatory elements in both E1a- and cyclic AMP-inducible promoters. Proc Natl Acad Sci USA 85:3396–3400.

Lonze BE, Ginty DD (2002) Function and regulation of CREB family transcription factors in the nervous system. Neuron 35:605–623.

Lowrey PL, Takahashi JS (2011) Genetics of Circadian Rhythms in Mammalian Model Organisms. In: Advances in Genetics, pp 175–230. Elsevier.

Low-Zeddies SS, Takahashi JS (2001) Chimera Analysis of the Clock Mutation in Mice Shows that Complex Cellular Integration Determines Circadian Behavior. Cell 105:25–42.

Lucas RJ, Freedman MS, Lupi D, Munoz M, David-Gray ZK, Foster RG (2001) Identifying the photoreceptive inputs to the mammalian circadian system using transgenic and retinally degenerate mice. Behavioural Brain Research 125:97–102.

Lucas RJ, Lall GS, Allen AE, Brown TM (2012) How rod, cone, and melanopsin photoreceptors come together to enlighten the mammalian circadian clock. In: Progress in Brain Research, pp 1–18. Elsevier.

Lungwitz E, Gannon RL (2009) Serotonin1A-mediated amplification of light-induced phase advances of circadian rhythms in the Syrian hamster: Post-light effects. Brain Research 1250:157–163.

Mai JK, Kedziora O, Teckhaus L, Sofroniew MV (1991) Evidence for subdivisions in the human suprachiasmatic nucleus. The Journal of Comparative Neurology 305:508–525.

Maywood ES, Mrosovsky N, Field MD, Hastings MH (1999) Rapid down-regulation of mammalian period genes during behavioral resetting of the circadian clock. Proceedings of the National Academy of Sciences 96:15211–15216.

McArthur AJ, Coogan AN, Ajpru S, Sugden D, Biello SM, Piggins HD (2000) Gastrin-releasing peptide phase-shifts suprachiasmatic nuclei neuronal rhythms in vitro. J Neurosci 20:5496–5502.

McCann KE, Sinkiewicz DM, Norvelle A, Huhman KL (2017) De novo assembly, annotation, and characterization of the whole brain transcriptome of male and female Syrian hamsters. Scientific Reports 7:40472.

Meijer JH, Robbers Y (2014) Wheel running in the wild. Proceedings of the Royal Society B: Biological Sciences 281:20140210–20140210.

Meijer JH, Rusak B, Gänshirt G (1992) The relation between light-induced discharge in the suprachiasmatic nucleus and phase shifts of hamster circadian rhythms. Brain Research 598:257–263.

Meijer JH, Schwartz WJ (2003) In Search of the Pathways for Light-Induced Pacemaker Resetting in the Suprachiasmatic Nucleus. Journal of Biological Rhythms 18:235–249.

Messager S, Ross AW, Barrett P, Morgan PJ (1999) Decoding photoperiodic time through Per1 and ICER gene amplitude. Proceedings of the National Academy of Sciences 96:9938–9943.

Meyer-Bernstein' EL, Morin LP (1996) Differential Serotonergic Innervation of the Suprachiasmatic Nucleus and the lntergeniculate Leaflet and its Role in Circadian Rhythm Modulation. J Neurosci:15.

Mielnicki LM, Pruitt SC (1991) Isolation and nucleotide sequence of a murine cDNA homologous to human activating transcription factor 4. Nucleic Acids Res 19:6332.

Mohamed HA, Yao W, Fioravante D, Smolen PD, Byrne JH (2005) cAMP-response Elements in Aplysia creb1, creb2, and Ap-uch Promoters: IMPLICATIONS FOR FEEDBACK LOOPS MODULATING LONG TERM MEMORY. Journal of Biological Chemistry 280:27035–27043.

Mohawk JA, Takahashi JS (2011) Cell autonomy and synchrony of suprachiasmatic nucleus circadian oscillators. Trends in Neurosciences 34:349–358.

Moore RY (2013) The Suprachiasmatic Nucleus and the Circadian Timing System. In: Progress in Molecular Biology and Translational Science, pp 1–28. Elsevier. Available at: http://linkinghub.elsevier.com/retrieve/pii/B9780123969712000014 [Accessed June 10, 2018].

Moore RY, Eichler VB (1972) Loss of a circadian adrenal corticosterone rhythm following suprachiasmatic lesions in the rat. Brain Res 42:201–206.

Moore RY, Lenn NJ (1972) A retinohypothalamic projection in the rat. J Comp Neurol 146:1–14.

Moore RY, Speh JC, Leak RK (2002) Suprachiasmatic nucleus organization. Cell and Tissue Research 309:89–98.

Morin LP (1994) The circadian visual system. Brain Research Reviews:26.

Moriya T, Horikawa K, Akiyama M, Shibata S (2000) Correlative Association betweenN-Methyl-D-Aspartate Receptor-Mediated Expression of Period Genes in the Suprachiasmatic Nucleus and Phase Shifts in Behavior with Photic Entrainment of Clock in Hamsters. Molecular Pharmacology 58:1554–1562.

Nagano M, Adachi A, Nakahama K, Nakamura T, Tamada M, Meyer-Bernstein E, Sehgal A, Shigeyoshi Y (2003) An abrupt shift in the day/night cycle causes desynchrony in the mammalian circadian center. J Neurosci 23:6141–6151.

Nakamura TJ, Fujimura K, Ebihara S, Shinohara K (2004) Light response of the neuronal firing activity in the suprachiasmatic nucleus of mice. Neuroscience Letters 371:244–248.

Nakamura W (2005) Differential Response of Period 1 Expression within the Suprachiasmatic Nucleus. Journal of Neuroscience 25:5481–5487.

Nakamura W, Honma S, Shirakawa T, Honma K (2002) Clock mutation lengthens the circadian period without damping rhythms in individual SCN neurons. Nature Neuroscience 5:399–400.

Niesler B, Walstab J, Combrink S, Möller D, Kapeller J, Rietdorf J, Bönisch H, Göthert M, Rappold G, Brüss M (2007) Characterization of the novel human serotonin receptor subunits 5-HT3C,5-HT3D, and 5-HT3E. Mol Pharmacol 72:8–17.

Nishikawa Y, Shibata S, Watanabe S (1995) Circadian changes in long-term potentiation of rat suprachiasmatic field potentials elicited by optic nerve stimulation in vitro. Brain Res 695:158–162.

Noguchi T, Watanabe K, Ogura A, Yamaoka S (2004) The clock in the dorsal suprachiasmatic nucleus runs faster than that in the ventral: Dorsal and ventral SCN clock differences. European Journal of Neuroscience 20:3199–3202.

Obrietan K, Impey S, Storm DR (1998) Light and circadian rhythmicity regulate MAP kinase activation in the suprachiasmatic nuclei. Nat Neurosci 1:693–700.

Pickard GE, Rea MA (1997) Serotonergic innervation of the hypothalamic suprachiasmatic nucleus and photic regulation of circadian rhythms. Biology of the Cell 89:513–523.

Piggins HD, Cutler DJ, Rusak B (1995) Ionophoretically applied substance P activates hamster suprachiasmatic nucleus neurons. Brain Research Bulletin 37:475–479.

Pittendrigh CS (1960) Circadian rhythms and the circadian organization of living systems. Cold Spring Harb Symp Quant Biol 25:159–184.

Pittendrigh CS (1993) Temporal organization: reflections of a Darwinian clock-watcher. Annu Rev Physiol 55:16–54.

Provencio I, Jiang G, De Grip WJ, Hayes WP, Rollag MD (1998) Melanopsin: An opsin in melanophores, brain, and eye. Proceedings of the National Academy of Sciences 95:340–345.

Ralph M, Foster R, David FC, Menaker M (1990) Transplanted Suprachiasmatic Nucleus Deternines Circadian Period. 247:5.

Ralph M, Menaker M (1988) A mutation of the circadian system in golden hamsters. Science 241:1225–1227.

Rea MA (1992) Different populations of cells in the suprachiasmatic nuclei express c-fos in association with light-induced phase delays and advances of the free-running activity rhythm in hamsters. Brain Research 579:107–112.

Rea MA, Barrera J, Glass JD, Gannon RL (1995) Serotonergic potentiation of photic phase shifts of the circadian activity rhythm. Neuroreport 6:1417–1420.

Rea MA, Glass JD, Colwell CS (1994) Serotonin modulates photic responses in the hamster suprachiasmatic nuclei. J Neurosci 14:3635–3642.

Rea MA, Pickard GE (2000) A 5-HT 1B receptor agonist inhibits light-induced suppression of pineal melatonin production. Brain Research 858:424–428.

Recio J, Pévet P, Masson-Pévet M (1996) Serotonergic modulation of photically induced increase in melatonin receptor density and Fos immunoreactivity in the suprachiasmatic nuclei of the rat. J Neuroendocrinol 8:839–845.

Reppert SM, Weaver DR (2001) Molecular Analysis of Mammalian Circadian Rhythms. Annual Review of Physiology 63:647–676.

Richter CP (1960) Biological Clocks in Medicine and Psychiatry: Shock-Phase Hypothesis. Proc Natl Acad Sci USA 46:1506–1530.

Ripperger JA, Jud C, Albrecht U (2011) The daily rhythm of mice. FEBS Letters 585:1384–1392.

Rosenwasser AM, Turek FW (2015) Neurobiology of Circadian Rhythm Regulation. Sleep Medicine Clinics 10:403–412.

Rusak B (1977) The role of the suprachiasmatic nuclei in the generation of circadian rhythms in the golden hamster,Mesocricetus auratus. Journal of Comparative Physiology ? A 118:145–164.

Rusak B, McNaughton L, Robertson HA, Hunt SP (1992) Circadian variation in photic regulation of immediate-early gene mRNAs in rat suprachiasmatic nucleus cells. Molecular Brain Research 14:124–130.

Sawaki Y, Nihonmatsu I, Kawamura H (1984) Transplantation of the neonatal suprachiasmatic nuclei into rats with complete bilateral suprachiasmatic lesions. Neuroscience Research 1:67–72.

Schmidt TM, Chen SK, Hattar S (2011) Intrinsically photosensitive retinal ganglion cells: many subtypes, diverse functions. Trends in Neurosciences 34:572–580.

Schurov IL, Hepworth TJ, Hastings MH (2002) Dopaminergic signalling in the rodent neonatal suprachiasmatic nucleus identifies a role for protein kinase A and mitogen-activated protein kinase in circadian entrainment. European Journal of Neuroscience 15:223–232.

Shearman LP, Zylka MJ, Weaver DR, Kolakowski LF, Reppert SM (1997) Two period homologs: circadian expression and photic regulation in the suprachiasmatic nuclei. Neuron 19:1261–1269.

Silver R, Lehman MN, Gibson M, Gladstone WR, Bittman EL (1990) Dispersed cell suspensions of fetal SCN restore circadian rhythmicity in SCN-lesioned adult hamsters. Brain Research 525:45–58.

Silver R, Romero MT, Besmer HR, Leak R, Nunez JM, LeSauter J (1996) Calbindin-D28K cells in the hamster SCN express light-induced Fos. Neuroreport 7:1224–1228.

Smart CM, Biello SM (2001) WAY-100635, a specific 5-HT1A antagonist, can increase the responsiveness of the mammalian circadian pacemaker to photic stimuli. Neurosci Lett 305:33–36.

Smith BN, Sollars PJ, Dudek FE, Pickard GE (2001) Serotonergic modulation of retinal input to the mouse suprachiasmatic nucleus mediated by 5-HT1B and 5-HT7 receptors. J Biol Rhythms 16:25–38.

Smith VM, Hagel K, Antle MC (2010) Serotonergic potentiation of photic phase shifts: examination of receptor contributions and early biochemical/molecular events. Neuroscience 165:16–27.

Smith VM, Jeffers RT, McAllister BB, Basu P, Dyck RH, Antle MC (2015a) Effects of lighting condition on circadian behavior in 5-HT1A receptor knockout mice. Physiology & Behavior 139:136–144.

Smith VM, Jeffers RT, Wu C, Vijaya Shankara J, Antle MC (2015b) Temporal changes of light-induced proteins in the SCN following treatment with the serotonin mixed agonist/antagonist BMY7378. Experimental Brain Research 233:2723–2731.

Smith VM, Sterniczuk R, Phillips CI, Antle MC (2008) Altered photic and non-photic phase shifts in 5-HT(1A) receptor knockout mice. Neuroscience 157:513–523.

Stephan FK, Zucker I (1972) Circadian Rhythms in Drinking Behavior and Locomotor Activity of Rats Are Eliminated by Hypothalamic Lesions. Proceedings of the National Academy of Sciences 69:1583–1586.

Sterniczuk R, Colijn MA, Nunez M, Antle MC (2010) Investigating the role of substance P in photic responses of the circadian system: Individual and combined actions with gastrin-releasing peptide. Neuropharmacology 58:277–285.

Sumová A, Illnerová H (2005) Effect of photic stimuli disturbing overt circadian rhythms on the dorsomedial and ventrolateral SCN rhythmicity. Brain Research 1048:161–169.

Takahashi JS (2016) Transcriptional architecture of the mammalian circadian clock. Nature Reviews Genetics 18:164–179.

Takumi T, Matsubara C, Shigeyoshi Y, Taguchi K, Yagita K, Maebayashi Y, Sakakida Y, Okumura K, Takashima N, Okamura H (1998) A new mammalian period gene predominantly expressed in the suprachiasmatic nucleus. Genes Cells 3:167–176.

Tanaka M, Hayashi S, Tamada Y, Ikeda T, Hisa Y, Takamatsu T, Ibata Y (1997) Direct retinal projections to GRP neurons in the suprachiasmatic nucleus of the rat. Neuroreport 8:2187–2191.

Tischkau SA, Mitchell JW, Tyan SH, Buchanan GF, Gillette MU (2003) Ca2+/cAMP Response Element-binding Protein (CREB)-dependent Activation of Per1 Is Required for Light-induced Signaling in the Suprachiasmatic Nucleus Circadian Clock. Journal of Biological Chemistry 278:718–723.

Travnickova Z, Sumova A, Peters R, Schwartz WJ, Illnerova H (1996) Photoperiod-dependent correlation between light-induced SCN c-fos expression and resetting of circadian phase. American Journal of Physiology-Regulatory, Integrative and Comparative Physiology 271:R825–R831.

Travnickova-Bendova Z, Cermakian N, Reppert SM, Sassone-Corsi P (2002) Bimodal regulation of mPeriod promoters by CREB-dependent signaling and CLOCK/BMAL1 activity. Proceedings of the National Academy of Sciences 99:7728–7733.

Tsujimoto A, Nyunoya H, Morita T, Sato T, Shimotohno K (1991) Isolation of cDNAs for DNA-binding proteins which specifically bind to a tax-responsive enhancer element in the long terminal repeat of human T-cell leukemia virus type I. J Virol 65:1420–1426.

Ueda HR, Hayashi S, Chen W, Sano M, Machida M, Shigeyoshi Y, Iino M, Hashimoto S (2005) System-level identification of transcriptional circuits underlying mammalian circadian clocks. Nature Genetics 37:187–192.

Vallejo M, Ron D, Miller CP, Habener JF (1993) C/ATF, a member of the activating transcription factor family of DNA-binding proteins, dimerizes with CAAT/enhancer-binding proteins and directs their binding to cAMP response elements. Proceedings of the National Academy of Sciences 90:4679–4683.

Van den Pol AN (1980) The hypothalamic suprachiasmatic nucleus of rat: intrinsic anatomy. J Comp Neurol 191:661–702.

van den Pol AN, Tsujimoto KL (1985) Neurotransmitters of the hypothalamic suprachiasmatic nucleus: immunocytochemical analysis of 25 neuronal antigens. Neuroscience 15:1049–1086.

Vogelbaum' MA, Menaker M (1992) Temporal Chimeras Produced by Hypothalamic Transplants. 12:3619–3627.

von Gall C, Duffield GE, Hastings MH, Kopp MD, Dehghani F, Korf HW, Stehle JH (1998) CREB in the mouse SCN: a molecular interface coding the phase-adjusting stimuli light, glutamate, PACAP, and melatonin for clockwork access. The Journal of neuroscience 18:10389–10397.

Weaver DR (1998) The Suprachiasmatic Nucleus: A 25-Year Retrospective. Journal of Biological Rhythms 13:100–112.

Weinert D, Fritzsche P, Gattermann R (2001) Activity rhythms of wild and laboratory golden hamsters (Mesocricetus auratus) under entrained and free-running conditions. Chronobiol Int 18:921–932.

Welsh DK, Logothetis DE, Meister M, Reppert SM (1995) Individual neurons dissociated from rat suprachiasmatic nucleus express independently phased circadian firing rhythms. Neuron 14:697–706.

Welsh DK, Takahashi JS, Kay SA (2010) Suprachiasmatic Nucleus: Cell Autonomy and Network Properties. Annual Review of Physiology 72:551–577.

Wilsbacher LD, Yamazaki S, Herzog ED, Song EJ, Radcliffe LA, Abe M, Block G, Spitznagel E, Menaker M, Takahashi JS (2002) Photic and circadian expression of luciferase in mPeriod1-luc transgenic mice in vivo. Proceedings of the National Academy of Sciences 99:489–494.

Wollnik F, Brysch W, Uhlmann E, Gillardon F, Bravo R, Zimmermann M, Schlingensiepen KH, Herdegen T (1995) Block of c-Fos and JunB Expression by Antisense Oligonucleotides Inhibits Light-induced-Phase Shifts of the Mammalian Circadian Clock. European Journal of Neuroscience 7:388–393.

Yamakawa GR, Antle MC (2010) Phenotype and function of raphe projections to the suprachiasmatic nucleus: Raphe projections to the suprachiasmatic nucleus. European Journal of Neuroscience 31:1974–1983.

Yan L, Okamura H (2002) Gradients in the circadian expression of Per1 and Per2 genes in the rat suprachiasmatic nucleus. European Journal of Neuroscience 15:1153–1162.

Yan L, Silver R (2002) Differential induction and localization of mPer1 and mPer2 during advancing and delaying phase shifts: Distinct role of mPer1 and mPer2 in phase shifts. European Journal of Neuroscience 16:1531–1540.

Yan L, Silver R (2004) Resetting the brain clock: time course and localization of mPER1 and mPER2 protein expression in suprachiasmatic nuclei during phase shifts: Light response of mPER1 and mPER2 in phase shifts. European Journal of Neuroscience 19:1105–1109.

Ying SW, Rusak B (1994) Effects of serotonergic agonists on firing rates of photically responsive cells in the hamster suprachiasmatic nucleus. Brain Research 651:37–46.

APPENDIX A

The use of siRNA *in vivo* is a new technique to be utilized in our laboratory, therefore a pilot experiment was run to assess if our protocol was effective in downregulating ATF4 expression in the SCN of Syrian Hamsters.

Methods Summary:

- Hamsters Housed in constant darkness (DD)
- Single intracranial SCN injections missense (10μg/1μL) siATF4 (10μg/1μL) at CT18
- No LP or Dim LP (15min at 40lux) given 24hrs following injection at CT18
- Part 1: Manipulations were done in the following order: 1) siATF4 only or siATF4+LP, 2) Missense only or Missense+LP, 3) counterbalanced Missense only or Missense+LP, and 4) counterbalanced siATF4 only or siATF4+LP (Figure A1, A3)
- Part 2: only the siATF4+LP (first) and Missense+LP (second) manipulations were done (Figure A2, A3)
- Histological evaluation using nissl stain

Conclusions:

- SiATF4 did not potentiate photic phase advances. However, there was huge variability in phase shifts observed. Some animals showed that siATF4 may be potentiating phase advances to light (~4hrs), while others did not. Some animals even potentiated phase advances to missense injections.
- Unclear 1) if concentration of siRNAs were effective, 2) if peak downregulation of siRNA occurs within 24hrs, and 3) if there were order effects between siRNA injections.

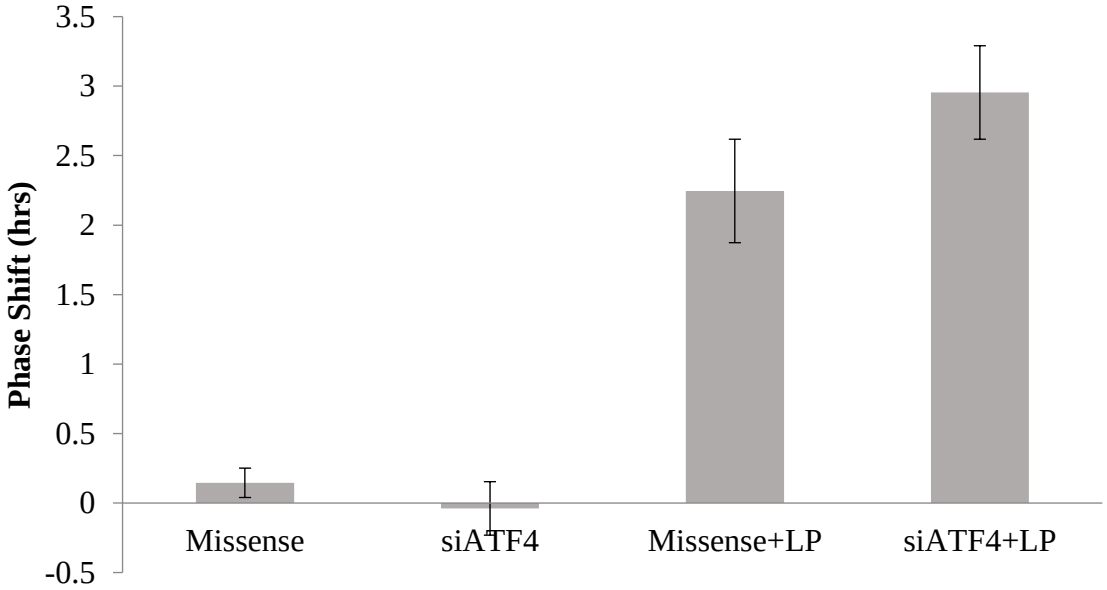

Figure A1. Mean phase shifts of hamsters (n=7) treated with either missense or siATF4 at CT18 24hrs prior to no LP or a 15 min LP (40lux) in a semi-counter balanced within-subjects design. Error bars signify ±SEM.

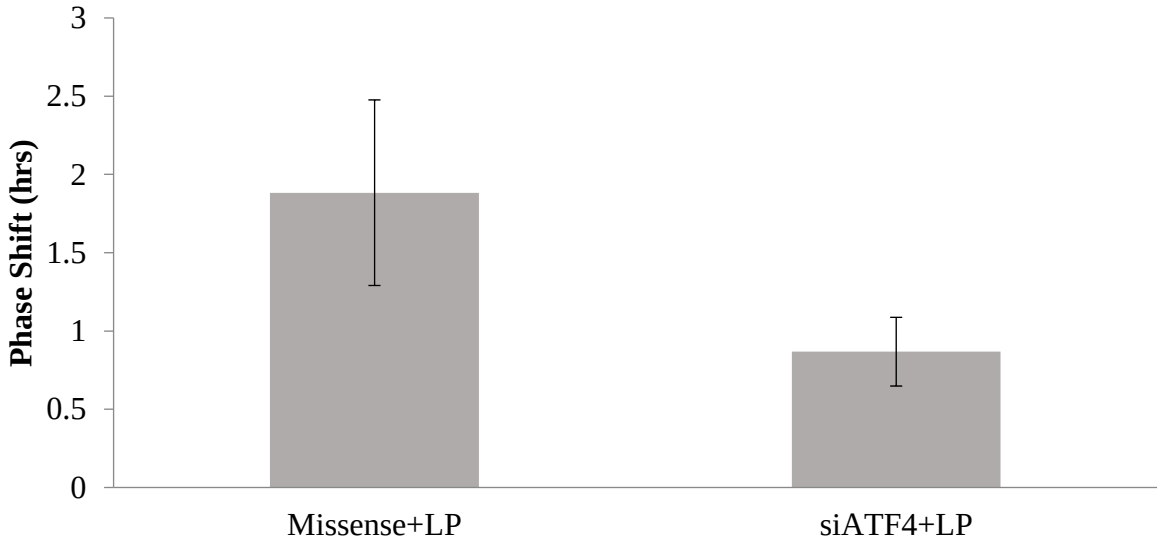

Figure A2. Mean phase shifts of hamsters (n=9) treated with either missense or siATF4 at CT18. 24hrs prior a 15 min LP (40lux) in an unbalanced within-subjects design. Error bars signify ±SEM.

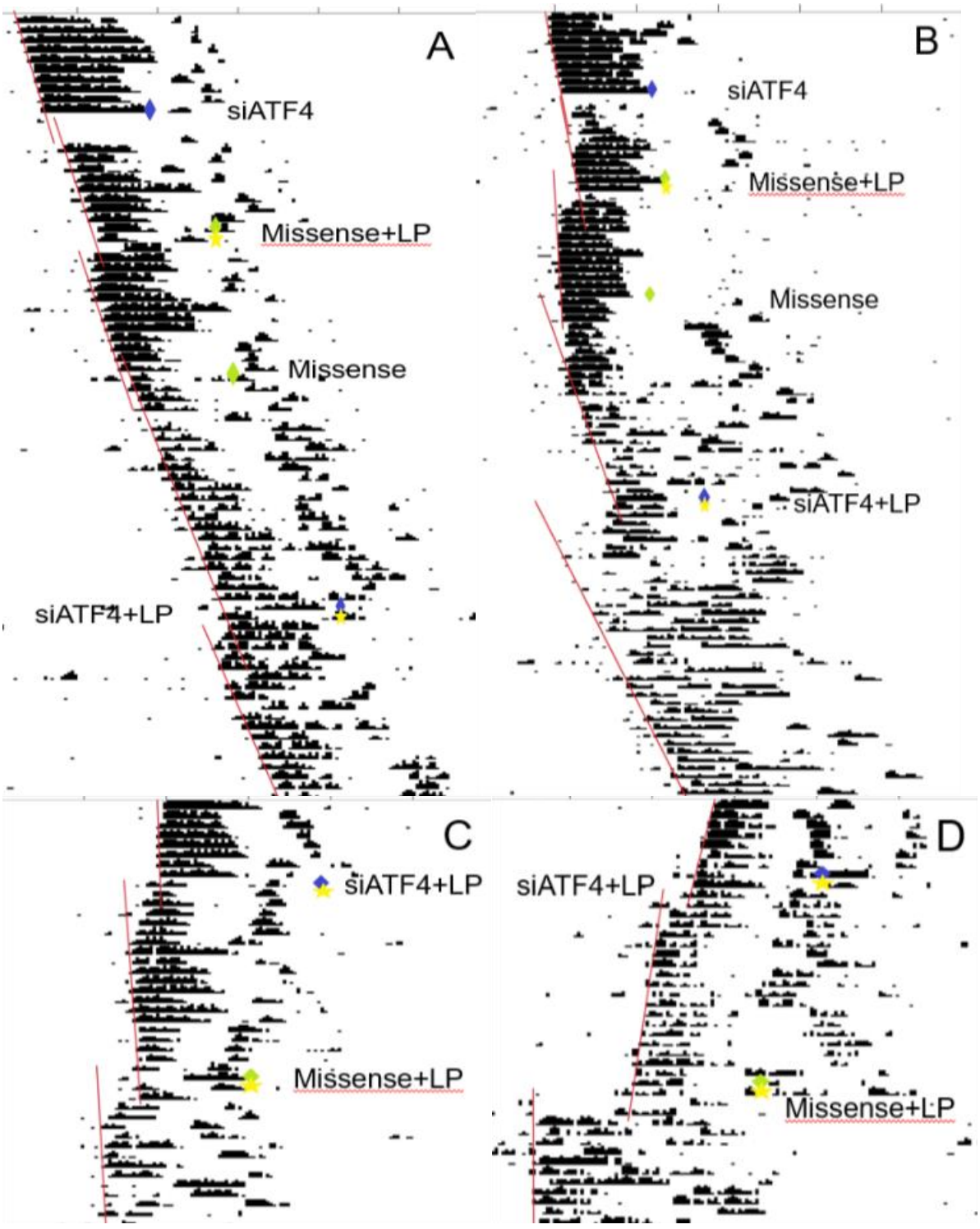

Figure A3. Actograms of four different hamsters. A and B are from the first round of injections in which the animals received all four treatments, while C and D are from the second round of injections in which the animals only received Missense+LP and siATF4+LP treatments. The green diamond represents missense injections, the blue diamond represents siATF4 injections, the yellow star represents the 15 min LP at 40 lux, and the red line represents a regression line of daily activity onsets.

APPENDIX B

To answer questions from the pilot experiment, a time-course experiment was implemented to investigate some of these factors.

Methods Summary:

- Hamsters were either given missense or siATF4 only.
- Three consecutive daily intracranial SCN injections missense (10μg/1μL) siATF4 (10μg/1μL) at any time
- Animals were also only given a LP (15min at 40lux) 1 day, 7 days, or 14 days (no LP/14 day conditions) following light exposure at a predicted CT18 (Figure B1, B2)
- ATF4 expression and cannula placement was evaluated using DAB-IHC (Figure B3, B4)

Conclusions:

- siATF4 injections followed by a LP 7 days after appeared to significantly potentiate phase advances compared to missense and at other time points.
- Phase advances appeared to begin after injections and may not be due to light exposure. It was postulated that siATF4 may be affecting endogenous rhythmicity
- DAB-IHC revealed that siATF4 did not significantly decrease the number of ATF4 expressing cells 1 day nor 7 days following injections, although were approaching significance.
- Decided to move forward with siRNA injection protocol with light exposure at 7 days after injections in an Aschoff Type 2 design to delineate rhythmic and photic effects of ATF4 downregulation of in the SCN.

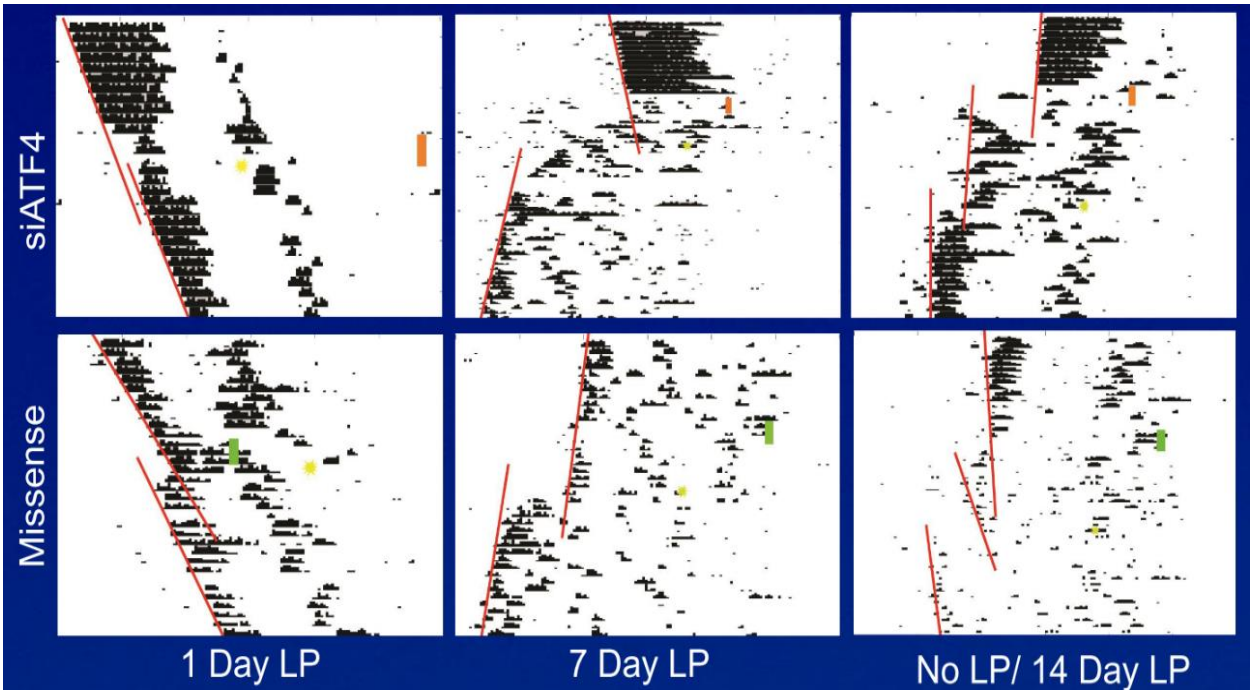

Figure B1. Actograms from three different hamsters each representing the two siRNA treatments with their assigned LP day following the injection. The orange rectangle represents the three siATF4 injections done over three days, the green rectangle represents the three Missense injections done over three days, the yellow star represents the 15 min LP at 40 lux, and the red line represents a regression line of daily activity onsets.

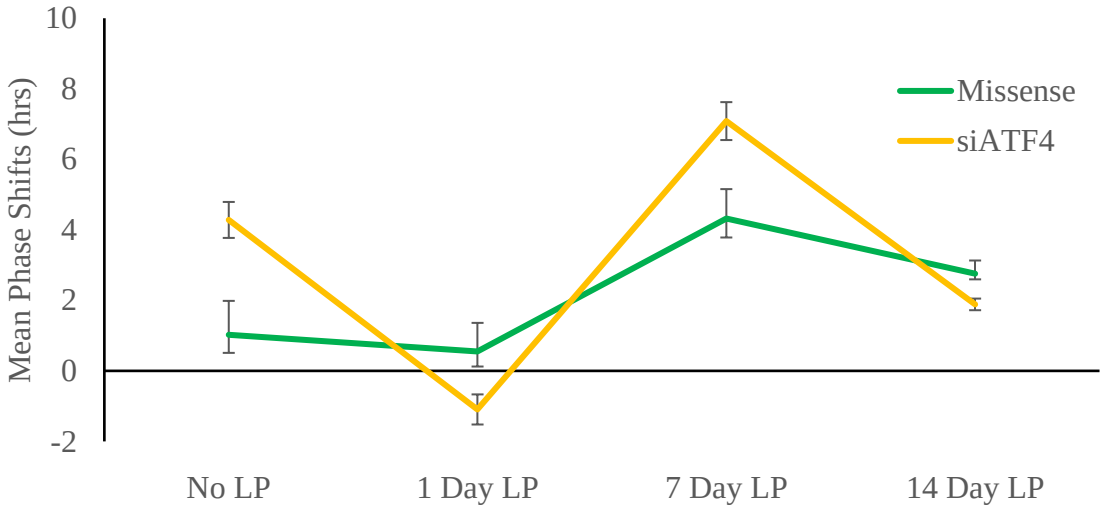

Figure B2. Mean phase shifts of hamsters (n=10) subjected to a phase advancing light pulse from the mixed factorial design siRNA time-course experiment. The within-subjects factor was the siRNA treatment (Missense or siATF4), while the between-subjects factor was the day in which the LP was presented to the animal: no LP (n=2), 1 Day LP (n=5), 7 Day LP (n=3), 14 Day LP (n=2). Error bars signify ±SEM.

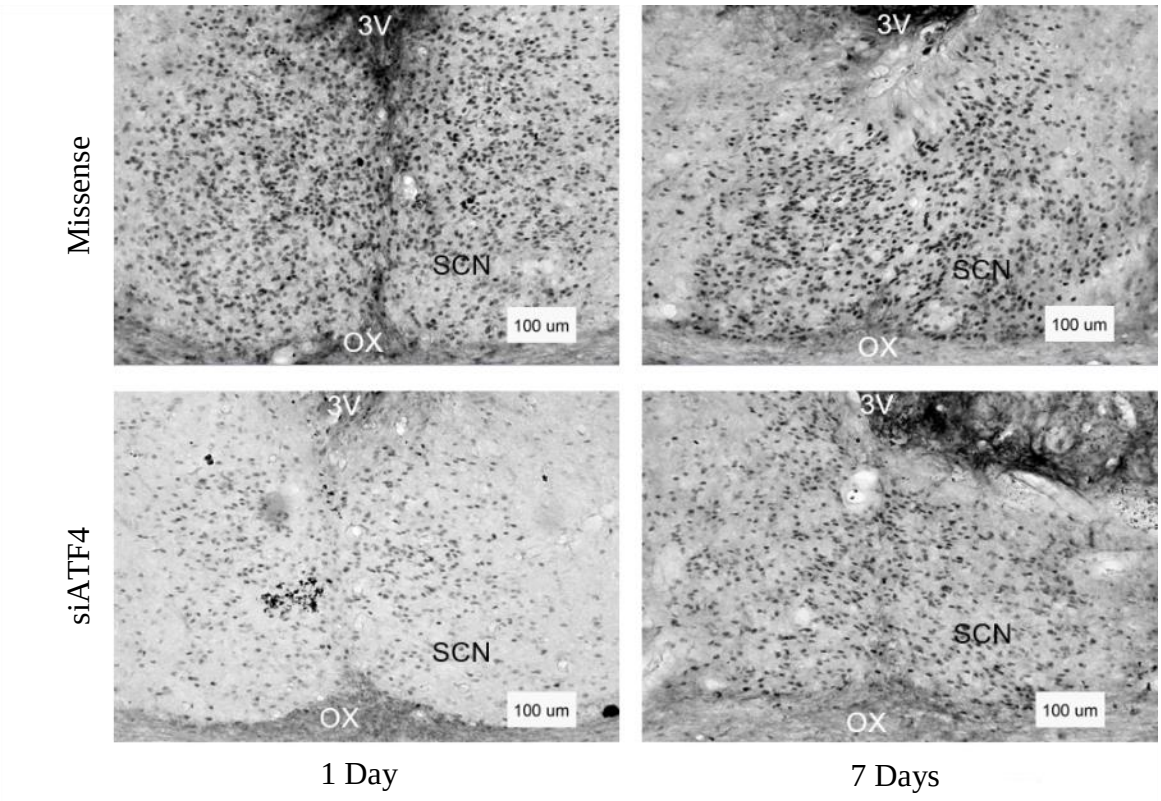

Figure B3. ATF4 expression using DAB-IHC to examine the number of ATF4 expression cells in the central-caudal SCN (coronal section) of four hamsters representing the four treatment groups: Missense+1D, Missense+7D, siATF4+1D, and siATF4+7D. SCN = suprachiasmatic nucleus, OX = optic chiasm, 3V = third ventricle. Scale bar = 100µm.

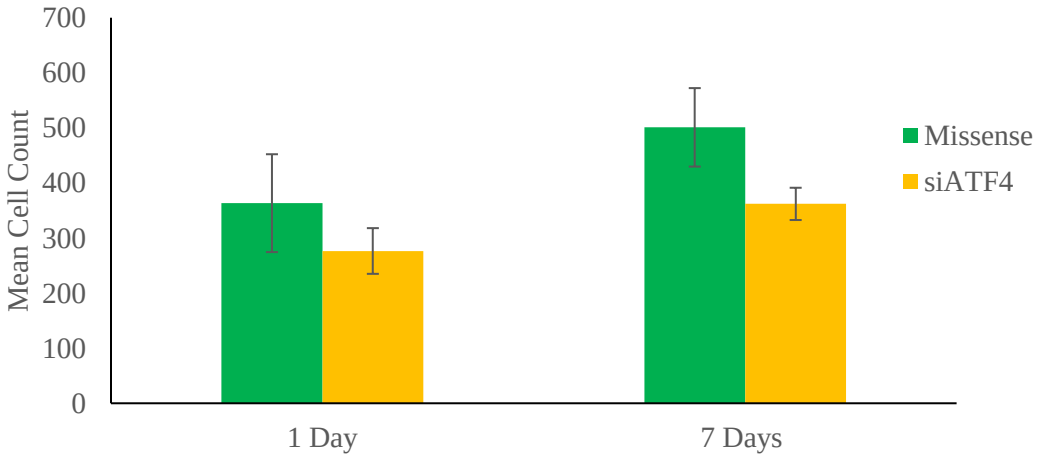

Figure B4. Mean cell count of ATF4 expressing cells in SCN of hamsters in the Missense+1D (n=3), siATF4+1D (n=2), Missense+7D (n=3), and siATF4+7D (n=3) conditions. Errors bars signify ±SEM.